NATIONAL ADVISORY COMMITTEE FOR AERONAUTICS

TECHNICAL NOTE 2454

JET-BOUNDARY CORRECTIONS FOR COMPLETE AND SEMISPAN SWEPT WINGS IN CLOSED CIRCULAR WIND TUNNELS

By James C. Sivells and Rachel M. Salmi

Langley Aeronautical Laboratory
Langley Field, Va.

Washington

September 1951

NATIONAL ADVISORY COMMITTEE FOR AERONAUTICS

TECHNICAL NOTE 2454

JET-BOUNDARY CORRECTIONS FOR COMPLETE AND SEMISPAN SWEPT WINGS IN CLOSED CIRCULAR WIND TUNNELS

By James C. Sivells and Rachel M. Salmi

SUMMARY

Tables and curves are presented which give values of the induced-upwash-velocity factors, due to the jet boundary, at the horizontal center plane of a closed circular wind tunnel and at that of a closed bipolar wind tunnel which is formed when a reflection plane is installed in a circular tunnel for testing semispan wings. These velocities have been calculated for infinitesimal-span lifting elements located at various points in the horizontal center plane. Inasmuch as the lift distribution of a wing of any plan form can be built up from the infinitesimal lifting elements, the induced upwash velocities can be obtained at any point on the wing or, to a limited extent, ahead of or behind the wing. The application of these induced-upwash-velocity factors to the determination of the jet-boundary corrections is also discussed. In order to facilitate the computations, simplified computing forms are presented for evaluating the corrections to the angle of attack and to the drag, pitching-moment, rolling-moment, and yawing-moment coefficients.

INTRODUCTION

Wind-tunnel testing of swept wings has considerably increased because of the use of such wings for transonic and supersonic aircraft. The jet-boundary corrections applicable to the test data on swept wings have been difficult to derive inasmuch as the problem is not reducible to that of a two-dimensional potential flow as in the case of unswept wings. For rectangular tunnels, the method of images can be used as in reference 1 for finite-span skewed horseshoe vortices, or as in reference 2 for infinitesimal-span lifting elements. For circular tunnels, there is no system of images that will satisfy the boundary conditions in the vicinity of the model. One method which has been developed for circular tunnels is given in reference 3 which follows the method of reference 4 and makes use of finite-span skewed horseshoe vortices.

The results of reference 3, however, have been found to be difficult to apply. Accordingly, the method presented herein was developed. This method makes use of infinitesimal-span lifting elements and is based upon the development given in reference 5.

For some purposes, such as lateral-control investigations, semi-span models are tested with reflection planes in order that larger models may be used in existing wind tunnels. Both the model and the tunnel are effectively reflected by the reflection plane. When one wall of a rectangular tunnel is used as a reflection plane, the effect is that of a complete model in a larger tunnel which is still rectangular. The corrections for such a configuration are given in reference 6. When a reflection plane is installed in a circular tunnel, however, the boundary of the complete tunnel (actual and reflected parts) is no longer circular, but consists of two circular arcs, the centers of which are equidistant from the reflection plane and on a line perpendicular to the reflection plane; this shape of tunnel is designated as bipolar. For such a tunnel, no rigorous method is available for determining the jet-boundary-induced upwash velocities at every point in the vicinity of the model. In the cross-sectional plane containing the infinitesimal lifting element, however, the boundary-induced velocities can be obtained by the two-dimensional analysis of reference 7. In order to obtain the induced velocities at other points, the assumption is made herein that the ratio of the induced velocity at a point in a plane ahead of or behind the lifting element to that at a corresponding point in the plane of the lifting element is the same in the bipolar tunnel as it is at the corresponding spanwise position in a circular tunnel. This assumption appears to be valid, at least on the tunnel center line, on the basis of comparisons made for tunnels of other shapes.

In addition to the determination of the jet-boundary-induced velocities, the method is presented herein for using these velocities in computing the corrections to be applied to the test data. Charts and tables are presented to simplify the computations and an example is given to illustrate their use. For the bipolar tunnel, only one location of the reflection plane is considered, but tables are given to facilitate the computations for other locations.

SYMBOLS

A	aspect ratio $\left(\frac{b^2}{S}\right)$
C_L	wing lift coefficient
C_l	corrected rolling-moment coefficient for complete wing

C_{l_c}	corrected rolling-moment coefficient for semispan wing
C_{l_s}	rolling-moment coefficient for semispan wing corrected for jet-boundary-induced angle but not for reflection-plane effect
C_{l_u}	uncorrected rolling-moment coefficient
ΔC_{D_j}	jet-boundary correction to drag coefficient
ΔC_{L_l}	induced lift coefficient acting on quarter-chord line
ΔC_{l_j}	jet-boundary correction to rolling-moment coefficient
ΔC_{l_r}	one-half reflection-plane correction to rolling-moment coefficient
C_m	pitching-moment coefficient
ΔC_{m_1}	correction to pitching-moment coefficient due to distortion of spanwise lift distribution
ΔC_{m_2}	correction to pitching-moment coefficient due to induced camber corresponding to the streamline curvature
ΔC_{m_j}	jet-boundary correction to wing pitching-moment coefficient
ΔC_{m_t}	additional correction to pitching-moment coefficient due to tail
ΔC_n	complete correction to yawing-moment coefficient
ΔC_{n_1}	reflection-plane correction to yawing-moment coefficient
ΔC_{n_2}	yawing-moment-coefficient correction due to jet-boundary-induced aileron upwash and wing-lift distribution
ΔC_{n_3}	yawing-moment-coefficient correction due to jet-boundary-induced wing upwash and aileron-lift distribution
F	jet-boundary-induced-upwash factor

F_c induced-upwash factor due to compensated potential

F_u induced-upwash factor due to uncompensated potential

$F_{+\sigma}$ jet-boundary-induced-upwash factor for positive value of σ

$F_{-\sigma}$ jet-boundary-induced-upwash factor for negative value of σ

J_m Bessel function of first kind of order m

J_m' first derivative of J_m with respect to its argument

M Mach number, ratio of free-stream velocity to sonic velocity

Q integral of upwash factor weighted by lift distribution (see computing tables)

S area of complete wing

V free-stream velocity

V' local velocity in vicinity of wing

V_t local velocity at tail

a three-dimensional lift-curve slope

a' fictitious lift-curve slope for antisymmetrical lift distributions $\left(\frac{2 + \sqrt{A^2\left(\beta^2 + \tan^2\Lambda_{0.25}\right) + 4}}{2 + \sqrt{A^2\left(\beta^2 + \tan^2\Lambda_{0.25}\right) + 16}}\, a\right)$

b span of complete wing

c section chord

$\bar{c}$ mean geometric chord (S/b)

c' mean aerodynamic chord $\left(\frac{2}{S}\int_0^{b/2} c^2 dy\right)$

c_l section lift coefficient

c_{l_b}	section lift coefficient for basic lift distribution
c_s	root chord
c_t	construction tip chord
h	tunnel height
i_t	incidence of tail, degrees
l_s	longitudinal distance from one-quarter-chord point on wing root chord to three-quarter-chord point on tail root chord
m	order of Bessel function
n	factor used in transformation of bipolar tunnel to circular tunnel
p	longitudinal coordinate of sink or doublet
q	free-stream dynamic pressure $\left(\frac{1}{2}\rho V^2\right)$
q_t	dynamic pressure at tail $\left(\frac{1}{2}\rho V_t^2\right)$
r	tunnel radius
s	lateral coordinate of lifting element
t	vertical coordinate of lifting element
w	jet-boundary-induced upwash velocity
w_c	induced upwash velocity due to compensated potential
w_0	jet-boundary-induced upwash velocity for infinitesimal lifting element
x	longitudinal coordinate
x_0	longitudinal distance from reference point to pitching-moment axis
x_1	longitudinal distance from reference point to centroid of induced lift on quarter-chord line

y	lateral coordinate
y_l	lateral distance to centroid of induced lift on quarter-chord line
z	vertical coordinate
Δz	jet-boundary correction due to wake displacement
Γ	strength of lifting element
Λ	sweep angle
Λ_0	sweep angle of leading edge of wing
Φ_u	uncompensated potential of a unit doublet
Ω_c	compensated potential of a unit sink
Ω_u	uncompensated potential of a unit sink
α_i	one-half the induced angle of the wing wake at infinity, radians
$\Delta\alpha_j$	jet-boundary correction to angle of attack, degrees
$\Delta\alpha_t$	additional jet-boundary-induced angle at tail, degrees $(\Delta\epsilon_t - \Delta\alpha_j)$
$\beta = \sqrt{1 - M^2}$	
γ	angle used in transformation of bipolar tunnel to circular tunnel, radians
$\Delta\epsilon_t$	jet-boundary correction to downwash angle at tail, degrees
ζ	nondimensional vertical coordinate (z/r for circular tunnel)
η	nondimensional lateral coordinate (y/r for circular tunnel)
θ	angular coordinate, cylindrical coordinate system
θ'	angular coordinate of lifting element
κ_s	factor in argument of Bessel functions
λ	taper ratio of wing (c_t/c_s)

ξ	nondimensional longitudinal coordinate (x/r)
ρ	mass density of air
σ	nondimensional lateral coordinate of lifting element (s/r for circular tunnel)
τ	ratio of increment in jet-boundary-induced upwash velocity to value at $\xi = 0$
ϕ_c	compensated potential for infinitesimal lifting element
ϕ_u	uncompensated potential (circular tunnel)
ϕ_a	additional potential
ϕ_u'	uncompensated potential (bipolar tunnel)
ω	radial coordinate, cylindrical coordinate system
ω'	radial coordinate of lifting element

Subscripts:

0.25	value along one-quarter-chord line
0.50	value along half-chord line
0.75	value along three-quarter-chord line
t	value for tail

DETERMINATION OF JET-BOUNDARY-INDUCED-VELOCITY FACTORS FOR INFINITESIMAL LIFTING ELEMENTS

Closed Circular Wind Tunnels

The development given in reference 5 makes use of the "uncompensated" potential ϕ_u of an infinitesimal lifting element in free air and the "compensated" potential ϕ_c of an infinitesimal lifting element in a wind tunnel. For a closed wind tunnel, the compensated potential must satisfy the condition of zero normal velocity at the jet boundary. The difference between these potentials $\phi_a = \phi_c - \phi_u$ is called the additional potential and must be a solution of Laplace's equation, must be regular throughout the field of motion, and must

vanish at an infinite distance upstream. For a circular tunnel, a function satisfying these conditions can be constructed with the aid of Bessel functions.

Another consideration which aids in the computation of the induced velocities is the fact, proved in reference 5, that the induced vertical velocity at a point (x,y,z) is equal to the difference between the value infinitely far downstream and the value at the point $(-x,y,z)$. In the following derivation, it is convenient to calculate values of induced velocity for negative values of x and subtract them from the values at infinity to obtain values for positive values of x.

The coordinate systems used hereinafter are shown in figure 1. The infinitesimal lifting element may be considered to be either a U-shaped vortex of infinitesimal span parallel to the y-axis with its trailing vortices parallel to the x-axis or a semi-infinite doublet line parallel to the x-axis with the axes of the doublets parallel to the z-axis. The potential of a doublet line may be derived from that of a sink (negative source) in the following manner. The uncompensated potential of a unit sink located at the point $(x=p,y=s,z=t)$ is given by the equation

$$\Omega_u = \frac{1}{4\pi} \frac{1}{\sqrt{(x - p)^2 + (y - s)^2 + (z - t)^2}} \tag{1}$$

The potential of a unit doublet with its axis vertical is obtained by differentiating equation (1) with respect to t,

$$\Phi_u = \frac{\partial \Omega_u}{\partial t} = \frac{z - t}{4\pi \left[(x - p)^2 + (y - s)^2 + (z - t)^2\right]^{3/2}} \tag{2}$$

The potential of the doublet line of lift $\rho V \Gamma \, ds$ is obtained by integrating equation (2) with respect to p and multiplying by $\Gamma \, ds$

$$\phi_u = \Gamma \, ds \int_0^\infty \Phi_u \, dp$$

$$\phi_u = \frac{\Gamma \, ds}{4\pi} \frac{z - t}{\sqrt{x^2 + (y - s)^2 + (z - t)^2} \left[\sqrt{x^2 + (y - s)^2 + (z - t)^2} - x\right]} \tag{3}$$

The compensated potential of a sink of strength 4π in a closed circular tunnel of radius r is given in reference 5 in cylindrical coordinates x, ω, and θ where $y = \omega \cos \theta$, $z = \omega \sin \theta$, $s = \omega' \cos \theta'$, and $t = \omega' \sin \theta'$. The compensated potential of a unit sink is given by the equation

$$\Omega_c = \frac{1}{\pi r^2} \sum_m {}' \sum_s \cos m(\theta - \theta') e^{-\kappa_s (p-x)} \frac{J_m(\kappa_s \omega) J_m(\kappa_s \omega')}{\left(1 - \frac{m^2}{\kappa_s^2 r^2}\right) \kappa_s J_m^2(\kappa_s r)} - \frac{p - x}{2\pi r^2} \tag{4}$$

where the J_m terms are Bessel functions of the first kind of order m. The summation with respect to m extends over all positive integers; the prime added to the $\sum$ sign indicates that a factor of $1/2$ must be inserted before the term corresponding to $m = 0$. The summation with respect to s for every m extends over all positive roots of the equation

$$J_m'(\kappa_s r) = 0$$

where $J_m'(\kappa_s r)$ is the derivative of the function $J_m(\kappa_s r)$ with respect to its argument. Equation (4) is valid only for positive values of $p - x$ so that it is valid for $p = 0$ and the negative values of x as used hereinafter.

By differentiating expression (4) with respect to t as in equation (2) and integrating with respect to p from 0 to ∞ as in equation (3), the compensated potential of the doublet line is obtained for $\theta' = 0$, $\omega' = s$, $t = 0$, as

$$\phi_c = \frac{\Gamma\, ds}{\pi r^2} \sum_m \sum_s e^{\kappa_s x} \sin m\theta \frac{m J_m(\kappa_s \omega) J_m(\kappa_s s)}{\left(1 - \frac{m^2}{\kappa_s^2 r^2}\right) \kappa_s^2 s \left[J_m(\kappa_s r)\right]^2} \tag{5}$$

The vertical velocity corresponding to the compensated potential is obtained by differentiating ϕ_c with respect to z. For the condition $\theta = 0$, $\omega = y$, $z = 0$, the vertical velocity is

$$w_c = \frac{\Gamma\, ds}{\pi r^2} \sum_m \sum_s e^{\kappa_s x} \frac{m^2 J_m(\kappa_s y) J_m(\kappa_s s)}{\left(1 - \frac{m^2}{\kappa_s^2 r^2}\right) \kappa_s^2 y s \left[J_m(\kappa_s r)\right]^2} \tag{6}$$

Using the substitution $F_c = \frac{\pi r^2 w_c}{\Gamma\, ds}$ and the nondimensional coordinates $\sigma = \frac{s}{r}$, $\eta = \frac{y}{r}$, and $\xi = \frac{x}{r}$ yields the equation

$$F_c = \sum_m \sum_s e^{\kappa_s r \xi} \frac{m^2 J_m(\kappa_s r \eta) J_m(\kappa_s r \sigma)}{\left(\kappa_s^2 r^2 - m^2\right) \eta \sigma \left[J_m(\kappa_s r)\right]^2} \tag{7}$$

The corresponding vertical-velocity factor for the uncompensated potential is found by differentiating equation (3) with respect to z. For the condition $z = 0$, $t = 0$,

$$F_u = \frac{1}{4\sqrt{\xi^2 + (\eta - \sigma)^2}\left[\sqrt{\xi^2 + (\eta - \sigma)^2} - \xi\right]} \tag{8}$$

The induced-vertical-velocity factor due to the jet boundary is the difference between that for the compensated potential and that for the uncompensated potential; that is,

$$F = F_c - F_u \tag{9}$$

Equations (7) and (8) are used only for negative values of ξ. Both equations become infinite for $\xi = 0$ and $\eta = \sigma$ but their difference, equation (9), is finite and equal to one-half the value at infinity (reference 5), which value is easily obtained as

$$F_{\xi=0} = \frac{1}{4(1 - \eta\sigma)^2} \tag{10}$$

Values of F for positive values of ξ are then obtained by the aforementioned relationship

$$F_{\xi>0} = 2F_{\xi=0} - F_{\xi<0} \tag{11}$$

Equations (7) to (11) have been evaluated over a range of ξ from -2.0 to 2.0, σ from -0.9 to 0.9, and η from 0 to 0.9, and the values of F are presented in table I. In evaluating equation (7), values of m up to 26 and s up to 16 were used where necessary to obtain convergence of the series to the desired number of decimal places. For $\xi = -0.2$ and $|\sigma|$ and η greater than 0.5, however, convergence was not obtained and the values of F given were interpolated. The values

of the Bessel functions used in equation (7) were obtained from reference 8.

For convenience in using the values of F as described hereinafter, the values of F were plotted against ξ and σ, and values of ξ and σ for constant values of F were obtained for the construction of the contours presented in figure 2. Values of F for negative values of η can be obtained by changing the sign of σ.

Closed Bipolar Wind Tunnels

When a reflection plane is installed in a circular wind tunnel for tests of semispan wings, the tunnel, as well as the model, is reflected. The complete tunnel, composed of that part of the circular tunnel containing the model and the reflected part containing the reflection of the model, becomes one of bipolar cross section as illustrated in figure 3. No rigorous method is available for determining the jet-boundary-induced velocities in a bipolar tunnel except at infinity, where the two-dimensional transformation of reference 7 can be used or in the plane $x = 0$, where the values of the induced vertical velocities are one-half the values at infinity. The assumption is therefore made herein that τ, the ratio of the increment in induced vertical velocity at any value of $\xi = \frac{x}{r}$ to the value for $\xi = 0$, is the same in the bipolar tunnel as it is in a circular tunnel for corresponding spanwise locations of the lifting element and the point at which the velocity is to be determined (where correspondence is determined by the conformal transformation of the circular to the bipolar shape). This assumption is believed to be approximately correct from a consideration of the results in reference 4 for circular and elliptic tunnels. When the values of τ for each shape of tunnel are plotted as a function of $2x/h$, good agreement is obtained, as shown in figure 4, along the longitudinal center line when the lifting element is located at the center of the tunnel. Similar agreement is indicated in reference 4 for other positions of the lifting element. Inasmuch as no transformation of position is necessary on the center line, comparisons can also be made with the values of τ for rectangular tunnels as shown in figure 4. The maximum increase in τ for the 2:1 tunnel over that of the square tunnel is about 20 percent. The maximum breadth-height ratio for a bipolar tunnel is 2:1, so that errors of the order of 20 percent may be involved in the aforementioned assumption. Such errors in the values of τ, however, would cause much smaller errors in the final jet-boundary corrections. Since the height of a bipolar tunnel is the same as that of the circular tunnel, it is assumed that the coordinate $\xi = \frac{x}{r}$ is the same for either tunnel. The other coordinates are indicated in figure 3 which represents the cross section of the bipolar

tunnel and the unit circle into which it is transformed infinitely far downstream where the two-dimensional conformal transformation is valid.

The transformation of reference 7 may be expressed as

$$\tan^{-1}(\eta + i\zeta) = n \tan^{-1} \frac{y + iz}{r \sin \gamma} \tag{12}$$

where

$$n = \frac{\pi}{2(\pi - \gamma)}$$

The distance η on the η-axis that corresponds to the distance y on the y-axis may be obtained by the relation

$$\tan^{-1}\eta = n \tan^{-1} \frac{y}{r \sin \gamma} \tag{13}$$

Similarly,

$$\tan^{-1}\sigma = n \tan^{-1} \frac{s}{r \sin \gamma} \tag{14}$$

The vortices due to an infinitesimal lifting element are of the same strength in each tunnel, but the distance ds between them in the bipolar tunnel is transformed to the distance $d\sigma$ in the circular tunnel where

$$d\sigma = \frac{n(1 + \sigma^2)ds}{r \sin \gamma \left(1 + \frac{s^2}{r^2 \sin^2 \gamma}\right)} \tag{15}$$

Although the reflection plane imposes the condition of symmetry about the vertical axis, it is convenient to calculate the induced velocities for positive s/r and later to add the velocities for negative s/r to obtain the symmetrical case. The uncompensated potential in the circular tunnel is

$$\phi_u = \frac{\Gamma \, d\sigma}{2\pi} \frac{\zeta}{(\eta - \sigma)^2 + \zeta^2} \tag{16}$$

The additional potential necessary to compensate for the effects of the boundary of the circular tunnel is due to image vortices located at $\frac{1}{\sigma}$ and may be expressed as

$$\phi_c - \phi_u = \frac{\Gamma\, d\sigma}{2\pi} \frac{\zeta}{(1 - \eta\sigma)^2 + \sigma^2\zeta^2} \tag{17}$$

The sum of equations (16) and (17) is the compensated potential in either the circular tunnel or the bipolar tunnel. The uncompensated potential in the bipolar tunnel is

$$\phi_u' = \frac{\Gamma\, ds}{2\pi} \frac{z}{(y - s)^2 + z^2} \tag{18}$$

The additional potential necessary to compensate for the effects of the boundary of the bipolar tunnel becomes

$$\phi_c - \phi_u' = \frac{\Gamma\, ds}{2\pi} \left[\frac{\zeta \frac{d\sigma}{ds}}{(\eta - \sigma)^2 + \zeta^2} + \frac{\zeta \frac{d\sigma}{ds}}{(1 - \eta\sigma)^2 + \sigma^2\zeta^2} - \frac{z}{(y - s)^2 + z^2} \right] \tag{19}$$

The vertical velocity in the plane $\xi = 0$ is

$$\frac{1}{2} \frac{\partial(\phi_c - \phi_u')}{\partial z}$$

which, for $z = 0$, is obtained as

$$w_0 = \frac{\Gamma\, ds}{4\pi} \left[\frac{\frac{\partial\zeta}{\partial z}\frac{d\sigma}{ds}}{(\eta - \sigma)^2} + \frac{\frac{\partial\zeta}{\partial z}\frac{d\sigma}{ds}}{(1 - \eta\sigma)^2} - \frac{1}{(y - s)^2} \right] \tag{20}$$

or

$$F_{\xi=0} = \frac{1}{4} \left[\frac{r^2 \frac{\partial\zeta}{\partial z}\frac{d\sigma}{ds}}{(\eta - \sigma)^2} + \frac{r^2 \frac{\partial\zeta}{\partial z}\frac{d\sigma}{ds}}{(1 - \eta\sigma)^2} - \frac{1}{\left(\frac{y}{r} - \frac{s}{r}\right)^2} \right] \tag{21}$$

where $\frac{d\sigma}{ds}$ is given by equation (15) and

$$\frac{\partial \zeta}{\partial z} = \frac{n(1 + \eta^2)}{r \sin \gamma \left(1 + \frac{y^2}{r^2 \sin^2 \gamma}\right)} \tag{22}$$

Equation (21) becomes indeterminate at the points $y = s$ or $\eta = \sigma$ but may be evaluated as

$$F_{\xi=0,y=s} = \frac{1}{4}\left[\frac{r^2 \frac{\partial \zeta}{\partial z}\frac{d\sigma}{ds}}{(1 - \eta\sigma)^2} - \frac{(1 - n)^2}{3 \sin^2 \gamma \left(1 + \frac{y^2}{r^2 \sin^2 \gamma}\right)^2}\right] \tag{23}$$

If τ is defined as

$$\tau = \frac{F_{\xi>0}}{F_{\xi=0}} - 1 \tag{24a}$$

or

$$\tau = 1 - \frac{F_{\xi<0}}{F_{\xi=0}} \tag{24b}$$

values of τ may be determined for a circular tunnel from the values of F in table I. The values of τ are assumed to be the same for a bipolar tunnel as for a circular tunnel. Equations (24) may also be used to determine values of F for the bipolar tunnel from the corresponding values of $F_{\xi=0}$. Values of τ are presented in table II for the symmetrical condition obtained by adding the values of F from table I for positive σ to the corresponding values for negative σ. Values of $F_{\xi=0}$ from equations (21) and (23) must be obtained for the same values of η and σ for which τ is obtained. The corresponding values of y/r and s/r are obtained from equations (13) and (14) and the values of $F_{\xi=0}$ for positive s/r are added to the corresponding values for negative s/r for the symmetrical condition. Contour plots of F obtained in this manner are presented in figure 5 for a position of the reflection plane equal to 0.49781r from the center line of a circular tunnel, corresponding to one of the values of reference 7.

DETERMINATION OF JET-BOUNDARY CORRECTIONS

Determination of Induced-Angle Distributions for Finite-Span Wing

The derivation of the jet-boundary corrections for swept wings follows, in many respects, that of reference 7 which is limited to unswept wings. The method of reference 7 was based upon the use of finite-span horseshoe vortices and necessitated that the spanwise lift distribution of the wing be broken into finite steps. Inasmuch as the method used herein is based upon the use of infinitesimal lifting elements, the jet-boundary-induced upwash angle, in radians, at any point on the model can be obtained by the relation

$$\frac{w}{V} = \frac{S}{4\pi r^2} \int_{-1}^{1} \frac{c_l c}{\bar{c}} F \, d\left(\frac{2s}{b}\right) \tag{25}$$

where the values of F are obtained from figure 2 or 5. The values of ξ, η, and σ (or ξ, y/r, and s/r) are so selected that the lifting element is located at the point where the lift is assumed to be acting, usually along the one-quarter-chord line of the wing.

If the spanwise lift distribution is symmetrical, equation (25) becomes, for the additional lift distribution,

$$\frac{w}{VC_L} = \frac{S}{4\pi r^2} \int_{0}^{1} \frac{c_l c}{C_L \bar{c}} \left(F_{+\sigma} + F_{-\sigma}\right) d\left(\frac{2s}{b}\right) \tag{26a}$$

and, for the basic lift distribution,

$$\frac{w}{V} = \frac{S}{4\pi r^2} \int_{0}^{1} \frac{c_{l_b} c}{\bar{c}} \left(F_{+\sigma} + F_{-\sigma}\right) d\left(\frac{2s}{b}\right) \tag{26b}$$

For convenience, figure 6, taken from reference 9, is presented herein for obtaining the additional loading coefficient $\frac{c_l c}{C_L \bar{c}}$ for use in equation (26a). The basic loading coefficient $\frac{c_{l_b} c}{\bar{c}}$ for twist due to aerodynamic washout or the deflection of partial-span flaps may be obtained by the approximate method of reference 10 or by the method of reference 9. The induced upwash angle given by equation (26b) is independent of lift coefficient and is usually small enough to be neglected.

If the spanwise lift distribution is antisymmetrical, due to aileron deflection, equation (25) becomes

$$\frac{w}{VC_l} = \frac{S}{4\pi r^2}\int_0^1 \frac{c_l c}{C_l \bar{c}} \left(F_{+\sigma} - F_{-\sigma}\right) d\left(\frac{2s}{b}\right) \tag{27}$$

For the reflection-plane condition, deflection of the ailerons produces a symmetrical lift distribution as if both ailerons of a complete wing were deflected in the same direction. For this case

$$\frac{w}{VC_l} = \frac{S}{4\pi r^2}\int_0^1 \frac{c_l c}{C_l \bar{c}} \left(F_{+\sigma} + F_{-\sigma}\right) d\left(\frac{2s}{b}\right) \tag{28}$$

The $\frac{c_l c}{C_l \bar{c}}$ distributions may be obtained by the approximate method of reference 10 or by the method of reference 11.

Compressibility Effects

First-order compressibility effects on the induced velocities and subsequent corrections can be readily taken into account by considering an equivalent wing in incompressible flow instead of the actual wing in compressible flow. The equivalent wing is obtained by multiplying all chordwise dimensions by $\frac{1}{\sqrt{1 - M^2}} = \frac{1}{\beta}$ according to the Glauert-Prandtl transformation. The aspect ratio of the equivalent wing then becomes equal to βA and the tangents of the sweep angles of the equivalent wing are $\frac{1}{\beta}$ times the tangents for the actual wing. Accordingly, in obtaining the values of F for use in equations (25) to (28), the values of ξ must be increased by the factor $\frac{1}{\beta}$. In these equations and subsequent ones, the lift distributions used should be those for the equivalent wing. Except for these modifications, the jet-boundary corrections are calculated for high-subsonic speeds (subcritical) in the same manner as for incompressible flow.

Derivations of Corrections

Angle of attack.- The jet-boundary correction to the angle of attack is due to the induced upwash angle at the three-quarter-chord line of the wing. In the vicinity of the wing, the induced upwash angle varies approximately linearly in the chordwise direction so that an effective camber of the circular-arc type is introduced by the jet

boundary. According to thin-airfoil theory the effective angle of attack for an airfoil with circular-arc camber is the angle at the three-quarter-chord point. The induced upwash angle at each point along the three-quarter-chord line is obtained according to equations (26). In order to obtain an average induced angle, which is the angle-of-attack correction, the local induced angle must be weighted according to the additional loading coefficient and then integrated along the span. This averaging procedure is proved in reference 10 for unswept wings and is at least approximately correct for swept wings also. For that part of the induced angle obtained by equation (26a), the angle-of-attack correction is given by the equation

$$\Delta\alpha_j = 57.3 C_L \int_0^1 \left(\frac{w}{VC_L}\right)_{0.75} \frac{c_l c}{C_L \bar{c}} \, d\left(\frac{2y}{b}\right) \tag{29}$$

The part of the induced angle obtained according to equation (26b) can be averaged in the same manner but the correction so determined is usually negligible.

The angle-of-attack correction obtained by equation (29) is added to the uncorrected or geometric angle of attack of the model.

Drag coefficient.- The jet-boundary correction to the drag coefficient is due to the inclination of the lift force by the induced upwash angle at the one-quarter-chord point. The correction to be added to the drag coefficient is the product of the lift coefficient and the average angle, in radians, along the one-quarter-chord line, or

$$\Delta C_{D_j} = C_L^2 \int_0^1 \left(\frac{w}{VC_L}\right)_{0.25} \frac{c_l c}{C_L \bar{c}} \, d\left(\frac{2y}{b}\right) \tag{30}$$

Wing pitching-moment coefficient.- A circularly cambered airfoil experiences (a) a lift, the centroid of which is at the one-quarter-chord point and the magnitude of which is given by the airfoil slope at the three-quarter-chord point, and (b) a pure couple, the magnitude of which is given by the camber. The jet-boundary correction to the swept-wing pitching-moment coefficient may be correspondingly considered as (a) the moment resulting from the outward shift in the spanwise center of lift caused by the induced washin along the three-quarter-chord line (this effect influences the pitching moment only for a swept wing) and (b) the couple due to the induced camber corresponding to the streamline curvature. The first correction may be determined by first determining the lift increment associated with the induced angle along the three-quarter-chord line

$$\Delta C_{L_1} = 57.3aC_L \int_0^1 \left(\frac{w}{VC_L}\right)_{0.75} \frac{c_l c}{C_L \bar{c}} \, d\left(\frac{2y}{b}\right) \tag{31}$$

and then determining the lateral center of pressure for this ΔC_{L_1}

$$\frac{2y_1}{b} \approx \frac{\frac{36.48a}{A}}{1 + \frac{36.48a}{A}} \int_0^1 \frac{c_l c}{C_L \bar{c}} \frac{2y}{b} \, d\left(\frac{2y}{b}\right) + \frac{\frac{57.3aC_L}{\Delta C_{L_1}}}{1 + \frac{36.48a}{A}} \int_0^1 \left(\frac{w}{VC_L}\right)_{0.75} \frac{c_l c}{C_L \bar{c}} \frac{2y}{b} \, d\left(\frac{2y}{b}\right) \tag{32}$$

which makes use of the approximation derived in reference 10 for the moment of the lift distribution due to twist. The longitudinal distance of this center of pressure x_1 can then be found from the wing geometry. Thus, if the root end of the one-quarter-chord line is used as a reference point,

$$\frac{x_1}{c'} = \frac{2y_1}{b} \frac{b}{2c'} \tan \Lambda_{0.25} \tag{33}$$

and the corresponding pitching-moment increment is

$$\Delta C_{m_1} = aC_L \frac{\Delta C_{L_1}}{aC_L} \frac{x_1 - x_0}{c'} \tag{34}$$

The correction ΔC_{m_2} due to the couple is

$$\Delta C_{m_2} = \frac{\pi \cos \Lambda_{0.50} \, C_L}{4} \int_0^1 \left[\left(\frac{w}{VC_L}\right)_{0.75} - \left(\frac{w}{VC_L}\right)_{0.25}\right] \frac{c^2}{c' \bar{c}} \, d\left(\frac{2y}{b}\right) \tag{35}$$

The total correction to the pitching-moment coefficient which is added to the uncorrected value is

$$\Delta C_{m_j} = \Delta C_{m_1} + \Delta C_{m_2} \tag{36}$$

Downwash angle.- For downwash surveys behind a wing, jet-boundary corrections must be applied to the measured downwash angles. The jet-boundary-induced upwash angle at any point in the horizontal center plane is found from equations (26) for which the lifting elements are located along the quarter-chord line of the wing and the additional lift distribution of the wing is used. For a specific tail location, the induced-upwash-angle distribution is found along the three-quarter-chord line of the tail and the average angle is obtained by the equation

$$\Delta\epsilon_t = 57.3C_L \int_0^1 \left(\frac{w}{VC_L}\right)_t \frac{V}{V_t}\left(\frac{c_l c}{C_L \bar{c}}\right)_t d\left(\frac{2y}{b_t}\right) \tag{37}$$

where $\frac{V}{V_t}$ is found from the air-flow surveys as $\frac{1}{\sqrt{q_t/q}}$. This angle is added to the average downwash measured by the air-flow surveys.

Wake displacement.- A jet-boundary correction must be applied to each vertical distance at which the downwash angle and dynamic pressure are measured by air-flow surveys in the tunnel. Longitudinal distributions of the induced upwash angle are obtained from equations (26) and the correction to the vertical distance is given by the equation

$$\Delta z = C_L \int_{T.E.}^{x} \left(\frac{w}{VC_L}\right) \frac{V}{V'} dx \tag{38}$$

where the integration is performed from the trailing edge of the wing to the point at which the measurements are made.

Pitching-moment coefficient (model with horizontal tail).- For a complete model with a horizontal tail, an additional jet-boundary correction must be applied to the pitching-moment coefficient because of the difference between the induced upwash angle at the tail and that at the wing. The additional induced angle at the tail is given by the equation

$$\Delta\alpha_t = \Delta\epsilon_t - \Delta\alpha_j \tag{39}$$

The additional jet-boundary correction, which is added to the previously corrected pitching-moment coefficient is given by the equation

$$\Delta C_{m_t} = \Delta\alpha_t \frac{dC_m}{di_t} \tag{40}$$

where $\frac{dC_m}{di_t}$ is the experimentally determined variation of pitching-moment coefficient with tail incidence.

Rolling-moment coefficient (circular tunnel).- The jet-boundary correction to the rolling-moment coefficient is the moment of the increment in the aileron lift distribution due to the induced upwash angle. For a circular tunnel this increment is antisymmetrical in the same manner as the lift distribution due to the deflected ailerons and its rolling-moment coefficient is given by the equation, based on the approximation of reference 10,

$$\Delta C_{l_j} = -\frac{C_{l_u}}{2}\frac{57.3a'}{1+\frac{18.24a'}{A}}\int_0^1\left(\frac{w}{VC_l}\right)_{0.75}\frac{c_l c}{C_L\bar{c}}\frac{2y}{b}\,d\left(\frac{2y}{b}\right) \tag{41}$$

where $\left(\frac{w}{VC_l}\right)_{0.75}$ is obtained by means of equation (27). The corrected value of the rolling-moment coefficient is

$$C_l = C_{l_u}\left(1+\frac{\Delta C_{l_j}}{C_{l_u}}\right) \tag{42}$$

Inasmuch as the correction is proportional to the measured rolling-moment coefficient, the same correction applies where only one aileron is deflected as well as where both ailerons are deflected, one up and one down.

Rolling-moment coefficient (bipolar tunnel).- Because of the symmetry imposed by the reflection plane for a semispan model, the increment in the aileron lift distribution, due to the induced upwash angle, is symmetrical. The rolling-moment coefficient of this increment is given by the equation

$$\Delta C_{l_j} = -\frac{C_{l_u}}{4}\frac{57.3a}{1+\frac{36.48a}{A}}\left[\frac{36.48a}{A}\int_0^1\left(\frac{w}{VC_l}\right)_{0.75}\frac{c_l c}{C_L\bar{c}}\,d\left(\frac{2y}{b}\right)\int_0^1\frac{c_l c}{C_L\bar{c}}\frac{2y}{b}\,d\left(\frac{2y}{b}\right)+\right.$$

$$\left.\int_0^1\left(\frac{w}{VC_l}\right)_{0.75}\frac{c_l c}{C_L\bar{c}}\frac{2y}{b}\,d\left(\frac{2y}{b}\right)\right] \tag{43}$$

which is also based upon the approximation of reference 10.

In addition to the jet-boundary correction, a reflection-plane correction must be applied to the rolling-moment coefficient for a semispan model. This reflection-plane correction $\frac{C_{l_c}}{C_{l_s}}$ is independent of the shape of the tunnel and is equal to the ratio of the rolling-moment coefficient per unit aileron deflection for a complete wing (antisymmetrical lift distribution) to that for a semispan model (symmetrical lift distribution). The reciprocal of this correction was first given for unswept wings in reference 12 as $1 + \frac{2\,\Delta C_{l_r}}{C_{l_c}}$ and may be also found in reference 7. The validity of the use of the unswept-wing values for swept wings has not been substantiated.

The completely corrected value of the rolling-moment coefficient is

$$C_{l_c} = C_{l_u}\left(1 + \frac{\Delta C_{l_j}}{C_{l_u}}\right)\frac{C_{l_c}}{C_{l_s}} \tag{44}$$

Yawing-moment coefficient (circular tunnel).- The jet-boundary corrections to the yawing-moment coefficient are defined as in reference 7 and are due to the interaction of the wing and aileron lift and induced-upwash-angle distributions. The equations for these corrections are

$$\Delta C_{n_2} = -\frac{C_L C_{l_u}}{2}\int_0^1 \left(\frac{w}{VC_l}\right)_{0.25}\frac{c_l c}{C_L \bar{c}}\frac{2y}{b}\,d\left(\frac{2y}{b}\right) \tag{45}$$

$$\Delta C_{n_3} = -\frac{C_L C_{l_u}}{2}\int_0^1 \left(\frac{w}{VC_L}\right)_{0.25}\frac{c_l c}{c_l \bar{c}}\frac{2y}{b}\,d\left(\frac{2y}{b}\right) \tag{46}$$

Theoretically, an additional correction, proportional to C_l^2 and due to the aileron lift and induced upwash angle, should be applied. This correction is usually negligible. The complete correction to be added to the uncorrected yawing-moment coefficient is

$$\Delta C_n = \Delta C_{n_2} + \Delta C_{n_3} \tag{47}$$

or, in terms of the corrected rolling-moment coefficient,

$$\Delta C_n = \frac{\frac{\Delta C_{n_2}}{C_L C_{l_u}} + \frac{\Delta C_{n_3}}{C_L C_{l_u}}}{1 + \frac{\Delta C_{l_j}}{C_{l_u}}} C_L C_l \tag{48}$$

Yawing-moment coefficient (bipolar tunnel).- For a bipolar tunnel, equations (45) and (46) become

$$\Delta C_{n_2} = -\frac{C_L C_{l_u}}{4} \int_0^1 \left(\frac{w}{V C_l}\right)_{0.25} \frac{c_l c}{C_L \bar{c}} \frac{2y}{b} \, d\left(\frac{2y}{b}\right) \tag{49}$$

and

$$\Delta C_{n_3} = -\frac{C_L C_{l_u}}{4} \int_0^1 \left(\frac{w}{V C_L}\right)_{0.25} \frac{c_l c}{C_l \bar{c}} \frac{2y}{b} \, d\left(\frac{2y}{b}\right) \tag{50}$$

In addition to the jet-boundary corrections, a reflection-plane correction must be applied to the yawing-moment coefficient for a semi-span model. This reflection-plane correction ΔC_{n_1} is independent of the shape of the tunnel and is equal to the difference between the self-induced yawing-moment coefficient per unit aileron deflection for a complete wing (antisymmetrical aileron distributions) and that for a complete wing (symmetrical aileron distributions) for the same lift coefficient. This correction was first given for unswept wings in reference 12 and reproduced in reference 7. As in the case of the reflection-plane correction for rolling-moment coefficient, the validity of the use of the unswept-wing values for swept wings has not been substantiated. The equation for ΔC_{n_1} is

$$\Delta C_{n_1} = -\frac{C_L C_{l_c}}{4} \int_0^1 \left(\frac{c_l c}{C_L \bar{c}} \frac{\alpha_i}{C_{l_c}} + \frac{c_l c}{C_{l_c} \bar{c}} \frac{\alpha_i}{C_L}\right) \frac{2y}{b} \, d\left(\frac{2y}{b}\right) +$$

$$\frac{C_L C_{l_s}}{4} \int_0^1 \left(\frac{c_l c}{C_L \bar{c}} \frac{\alpha_i}{C_{l_s}} + \frac{c_l c}{C_{l_s} \bar{c}} \frac{\alpha_i}{C_L}\right) \frac{2y}{b} \, d\left(\frac{2y}{b}\right) \tag{51}$$

where C_{l_c} is used to identify the distributions of lift and induced angle (in radians) for a complete model and C_{l_s} is used to identify

those for a semispan model. The method of reference 13 can be used to determine α_i from the spanwise lift distributions of swept wings even though this method was developed for unswept wings.

The complete correction to be added to the uncorrected yawing-moment coefficient is

$$\Delta C_n = \Delta C_{n_1} + \Delta C_{n_2} + \Delta C_{n_3} \tag{52}$$

or, in terms of the corrected rolling-moment coefficient,

$$\Delta C_n = \left[\frac{\Delta C_{n_1}}{C_L C_{l_c}} + \frac{\dfrac{\Delta C_{n_2}}{C_L C_{l_u}} + \dfrac{\Delta C_{n_3}}{C_L C_{l_u}}}{\left(1 + \dfrac{\Delta C_{l_j}}{C_{l_u}}\right)\dfrac{C_{l_c}}{C_{l_s}}} \right] C_L C_{l_c} \tag{53}$$

ILLUSTRATIVE EXAMPLE

In order to illustrate the procedure involved in the computation of the jet-boundary corrections, the corrections for a complete model in a circular tunnel are now determined. The determination of the corrections for a semispan model in a bipolar tunnel would be very similar except for the corrections to the rolling- and yawing-moment coefficients where equations (43), (49), and (50) must be used instead of equations (41), (45), and (46) and for the corrections to the rolling-moment and yawing-moment coefficients due to the reflection plane.

For the example illustrated, the wing had a leading-edge sweepback of 47.72°, an aspect ratio of 5.11, and a taper ratio of 0.383 and the tail had a sweepback of 44.29° at the quarter-chord line, an aspect ratio of 4.01, and a taper ratio of 0.625 and was located with respect to the wing so that the distance between the one-quarter-chord point of the wing root chord and the three-quarter-chord point of the tail root chord was 0.787 times the tunnel radius. The constants used in the computations are given in table III.

In all the computations involving integrations, numerical integration is used. The integrating multipliers at the four spanwise stations used were determined by means of an application of Simpson's (parabolic) rule in the same manner as that described in reference 13. The four spanwise stations are those for which the values of loading coefficient are given in figure 6 and are equally spaced with respect to the angle $\cos^{-1}\frac{2y}{b}$. The symmetrical lift distributions for the wing and tail were obtained from figure 6 and the antisymmetrical lift distribution for the wing with deflected ailerons was obtained by the approximate method of reference 10.

Computation of Jet-Boundary-Induced Angle

Tables IV to IX present the computation of the jet-boundary-induced-angle distributions along the one-quarter-chord line of the wing, along the three-quarter-chord line of the wing, and along the three-quarter-chord line of the tail. In table IV, the values of σ correspond to the spanwise stations at which the values of the loading coefficient are obtained from figure 6. For each combination of σ and η, the values of ξ are determined by the equations given at the bottom of table IV and the corresponding values of F are obtained from figure 2 and tabulated in table IV. In tables V to VII, the values of F for negative σ are added to the values for positive σ and the values of $\frac{w}{VC_L}$ are obtained according to equation (26a). Table V is for the one-quarter-chord line of the wing, table VI is for the three-quarter-chord line of the wing, and table VII is for the three-quarter-chord line of the tail. The values of $\frac{w}{VC_L}$ thus obtained are plotted in figure 7 as a function of $\frac{\eta}{\eta_{max}}$ which is equal to $\frac{2y}{b}$. In table VIII and IX, the values of F for negative σ are subtracted from the values for positive σ and the values of $\frac{w}{VC_l}$ are obtained according to equation (27). Table VIII is for the one-quarter-chord line of the wing and table IX is for the three-quarter-chord line. The values of $\frac{w}{VC_l}$ thus obtained are plotted in figure 8.

Computation of Jet-Boundary Corrections

Angle of attack and drag coefficient.- Table X presents the computation of the jet-boundary corrections to the angle of attack and to the drag coefficient according to equations (29) and (30), respectively. For this table, the values of $\frac{w}{VC_L}$ are read from figure 7 at each of the spanwise stations for which values of the loading coefficient have been obtained.

Pitching-moment coefficient.- Table XI presents the computation of the jet-boundary correction to the pitching-moment coefficient for the wing-alone case according to equation (36). The values of $\left(\frac{w}{VC_L}\right)_{0.75}$ and $\left(\frac{w}{VC_L}\right)_{0.75} - \left(\frac{w}{VC_L}\right)_{0.25}$ are obtained from the values given in table X. Values of ΔC_{L_1}, $\frac{2y_1}{b}$, and $\frac{x_1}{c'}$ are obtained according to equations (31) and (33), respectively. The value of $\frac{x_0}{c'}$ is given and the value of ΔC_{m_1} can be obtained according to equation (34). For the purpose of determining this correction, the experimental value of the wing lift-curve slope a should be used. Sufficient accuracy is obtained, however, by using the approximate value of a as given by the equation

$$a \approx \frac{0.1097A}{2 + \sqrt{A^2\left(\beta^2 + \tan^2\Lambda_{0.25}\right) + 4}} \tag{54}$$

which includes the edge-velocity factor as used in reference 10 for symmetrical lift distributions, but modified for compressibility effects. The value of ΔC_{m_2} is given by equation (35).

Table XII presents the computation of the jet-boundary correction to the downwash angle according to equation (37) and the additional correction to the pitching-moment coefficient for the wing-plus-tail configuration according to equations (39) and (40).

Rolling-moment and yawing-moment coefficients.- Table XIII presents the computation of the jet-boundary corrections to the rolling-moment coefficient according to equations (41) and (42) and to the yawing-moment coefficient according to equations (45) to (48). The approximate value of a' given by the equation

$$a' \approx \frac{0.1097A}{2 + \sqrt{A^2\left(\beta^2 + \tan^2\Lambda_{0.25}\right) + 16}} \tag{55}$$

is used in equation (41).

For a semispan model in a bipolar tunnel, the moment multipliers in column (10) must be divided by 2 to take into account the different constants in the denominators of the equations for ΔC_{l_j}, ΔC_{n_2}, and ΔC_{n_3}. Furthermore, equation (43) must be used instead of equation (41) and the reflection-plane corrections must be added.

CONCLUDING REMARKS

A method is presented for determining the jet-boundary corrections to be applied to test data for complete and semispan swept wings in closed circular wind tunnels. The corrections for angle of attack and for drag, pitching-moment, rolling-moment, and yawing-moment coefficients are illustrated in detail in simplified computing forms.

Langley Aeronautical Laboratory
National Advisory Committee for Aeronautics
Langley Field, Va., March 21, 1951

REFERENCES

1. Swanson, Robert S.: Jet-Boundary Corrections to a Yawed Model in a Closed Rectangular Wind Tunnel. NACA ARR, Feb. 1943.

2. Katzoff, S., and Hannah, Margery E.: Calculation of Tunnel-Induced Upwash Velocities for Swept and Yawed Wings. NACA TN 1748, 1948.

3. Eisenstadt, Bertram J.: Boundary-Induced Upwash for Yawed and Swept-Back Wings in Closed Circular Wind Tunnels. NACA TN 1265, 1947.

4. Lotz, Irmgard: Correction of Downwash in Wind Tunnels of Circular and Elliptic Sections. NACA TM 801, 1936.

5. Von Kármán, Th., and Burgers, J. M.: General Aerodynamic Theory - Perfect Fluids. Influence of Boundaries in the Field of Motion around Airfoil Systems. Vol. II of Aerodynamic Theory, div. E, ch. IV, sections 42 to 44, W. F. Durand, ed., Julius Springer (Berlin), 1935, pp. 266-273.

6. Polhamus, Edward C.: Jet-Boundary-Induced-Upwash Velocities for Swept Reflection-Plane Models Mounted Vertically in 7- by 10-Foot, Closed, Rectangular Wind Tunnels. NACA TN 1752, 1948.

7. Sivells, James C., and Deters, Owen J.: Jet-Boundary and Plan-Form Corrections for Partial-Span Models with Reflection Plane, End Plate, or No End Plate in a Closed Circular Wind Tunnel. NACA Rep. 843, 1946. (Formerly NACA TN 1077.)

8. Staff of the Computation Laboratory: The Annals of the Computation Laboratory of Harvard University. Tables of the Bessel Functions of the First Kind of Orders Zero to Twenty-Seven. Vols. III-IX, Harvard Univ. Press, 1947-48.

9. DeYoung, John, and Harper, Charles W.: Theoretical Symmetric Span Loading at Subsonic Speeds for Wings Having Arbitrary Plan Form. NACA Rep. 921, 1948.

10. Sivells, James C.: An Improved Approximate Method for Calculating Lift Distributions Due to Twist. NACA TN 2282, 1951.

11. DeYoung, John: Theoretical Antisymmetric Span Loading for Wings of Arbitrary Plan Form at Subsonic Speeds. NACA TN 2140, 1950.

12. Swanson, Robert S., and Toll, Thomas A.: Jet-Boundary Corrections for Reflection-Plane Models in Rectangular Wind Tunnels. NACA Rep. 770, 1943. (Formerly NACA ARR 3E22.)

13. Sivells, James C., and Westrick, Gertrude C.: Method for Calculating Lift Distributions for Unswept Wings with Flaps or Ailerons by Use of Nonlinear Section Lift Data. NACA TN 2283, 1951.

TABLE I.- BOUNDARY-INDUCED-UPWASH FACTOR, $F = \frac{\pi r w_0}{\Gamma \, d\sigma}$, AT POINTS (ξ,η) DUE TO INFINITESIMAL LIFTING ELEMENTS LOCATED AT POINTS $(0,\sigma)$

(a) $\eta = 0$

ξ	F										
	$\sigma = -0.9$	$\sigma = -0.8$	$\sigma = -0.7$	$\sigma = -0.5$	$\sigma = -0.2$	$\sigma = 0$	$\sigma = 0.2$	$\sigma = 0.5$	$\sigma = 0.7$	$\sigma = 0.8$	$\sigma = 0.9$
-2.0	-0.0079	-0.0070	-0.0062	-0.0049	-0.0036	-0.0034	-0.0036	-0.0049	-0.0062	-0.0070	-0.0079
-1.8	-.0062	-.0050	-.0040	-.0022	-.0007	-.0003	-.0007	-.0022	-.0040	-.0050	-.0062
-1.6	-.0015	.0001	.0016	.0040	.0062	.0066	.0062	.0040	.0016	.0001	.0015
-1.4	.0060	.0083	.0103	.0136	.0165	.0170	.0165	.0136	.0103	.0083	.0060
-1.2	.0176	.0206	.0233	.0275	.0312	.0319	.0312	.0275	.0233	.0206	.0176
-1.0	.0348	.0386	.0419	.0471	.0515	.0523	.0515	.0471	.0419	.0386	.0348
-.8	.0594	.0639	.0677	.0735	.0784	.0793	.0784	.0735	.0677	.0639	.0594
-.6	.0932	.0979	.1018	.1077	.1124	.1133	.1124	.1077	.1018	.0979	.0932
-.4	.1373	.1414	.1447	.1496	.1535	.1542	.1535	.1496	.1447	.1414	.1373
-.2	.1908	.1932	.1951	.1980	.2001	.2007	.2001	.1980	.1951	.1932	.1908
0	.2500	.2500	.2500	.2500	.2500	.2500	.2500	.2500	.2500	.2500	.2500
.2	.3092	.3068	.3049	.3020	.2999	.2993	.2999	.3020	.3049	.3068	.3092
.4	.3627	.3586	.3553	.3504	.3465	.3458	.3465	.3504	.3553	.3586	.3627
.6	.4068	.4021	.3982	.3923	.3876	.3867	.3876	.3923	.3982	.4021	.4068
.8	.4406	.4361	.4323	.4265	.4216	.4207	.4216	.4265	.4323	.4361	.4406
1.0	.4652	.4614	.4581	.4529	.4485	.4477	.4485	.4529	.4581	.4614	.4652
1.2	.4824	.4794	.4767	.4725	.4688	.4681	.4688	.4725	.4767	.4794	.4824
1.4	.4940	.4917	.4897	.4864	.4835	.4830	.4835	.4864	.4897	.4917	.4940
1.6	.5015	.4999	.4984	.4960	.4938	.4934	.4938	.4960	.4984	.4999	.5015
1.8	.5062	.5050	.5040	.5022	.5007	.5003	.5007	.5022	.5040	.5050	.5062
2.0	.5079	.5070	.5062	.5049	.5036	.5034	.5036	.5049	.5062	.5070	.5079

TABLE I.- BOUNDARY-INDUCED-UPWASH FACTOR F - Continued

(b) $\eta = 0.2$

ξ	F										
	$\sigma = -0.9$	$\sigma = -0.8$	$\sigma = -0.7$	$\sigma = -0.5$	$\sigma = -0.2$	$\sigma = 0$	$\sigma = 0.2$	$\sigma = 0.5$	$\sigma = 0.7$	$\sigma = 0.8$	$\sigma = 0.9$
-2.0	-0.0074	-0.0067	-0.0060	-0.0048	-0.0038	-0.0036	-0.0040	-0.0054	-0.0069	-0.0078	-0.0088
-1.8	-.0058	-.0048	-.0039	-.0024	-.0009	-.0007	-.0010	-.0027	-.0046	-.0058	-.0071
-1.6	-.0015	-.0001	.0012	.0034	.0056	.0062	.0060	.0038	.0013	-.0004	-.0022
-1.4	.0051	.0071	.0090	.0121	.0154	.0165	.0164	.0140	.0107	.0085	.0059
-1.2	.0150	.0177	.0202	.0246	.0294	.0312	.0317	.0293	.0253	.0225	.0192
-1.0	.0291	.0326	.0358	.0417	.0484	.0515	.0530	.0516	.0474	.0441	.0400
-.8	.0483	.0526	.0567	.0642	.0735	.0784	.0817	.0827	.0794	.0763	.0718
-.6	.0734	.0785	.0834	.0927	.1051	.1124	.1186	.1244	.1243	.1224	.1190
-.4	.1044	.1101	.1157	.1267	.1429	.1535	.1636	.1773	.1836	.1853	.1854
-.2	.1397	.1473	.1526	.1672	.1854	.2001	.2151	.2418	.2566	.2652	.2726
0	.1795	.1858	.1924	.2066	.2311	.2500	.2713	.3086	.3380	.3543	.3718
.2	.2194	.2243	.2321	.2461	.2769	.2999	.3275	.3755	.4195	.4434	.4710
.4	.2547	.2615	.2690	.2865	.3194	.3465	.3789	.4400	.4924	.5233	.5582
.6	.2857	.2931	.3013	.3206	.3572	.3876	.4240	.4929	.5517	.5862	.6246
.8	.3108	.3189	.3280	.3490	.3887	.4216	.4609	.5346	.5966	.6324	.6718
1.0	.3300	.3390	.3489	.3716	.4138	.4485	.4896	.5657	.6287	.6645	.7036
1.2	.3441	.3539	.3645	.3887	.4329	.4688	.5109	.5880	.6507	.6861	.7244
1.4	.3539	.3645	.3758	.4011	.4469	.4835	.5261	.6033	.6654	.7001	.7377
1.6	.3606	.3717	.3835	.4098	.4566	.4938	.5366	.6134	.6748	.7090	.7458
1.8	.3649	.3764	.3887	.4156	.4632	.5007	.5435	.6200	.6807	.7144	.7507
2.0	.3665	.3782	.3907	.4180	.4661	.5036	.5465	.6227	.6829	.7164	.7524

TABLE I.- BOUNDARY-INDUCED-UPWASH FACTOR F - Continued

(c) $\eta = 0.5$

ξ	F										
	$\sigma = -0.9$	$\sigma = -0.8$	$\sigma = -0.7$	$\sigma = -0.5$	$\sigma = -0.2$	$\sigma = 0$	$\sigma = 0.2$	$\sigma = 0.5$	$\sigma = 0.7$	$\sigma = 0.8$	$\sigma = 0.9$
-2.0	-0.0074	-0.0068	-0.0063	-0.0055	-0.0048	-0.0049	-0.0054	-0.0071	-0.0089	-0.0099	-0.0111
-1.8	-.0061	-.0053	-.0047	-.0035	-.0024	-.0015	-.0027	-.0046	-.0069	-.0083	-.0098
-1.6	-.0025	-.0014	-.0004	.0014	.0034	.0040	.0038	.0017	-.0012	-.0031	-.0053
-1.4	.0028	.0044	.0059	.0087	.0121	.0136	.0140	.0121	.0086	.0060	.0029
-1.2	.0105	.0127	.0149	.0190	.0246	.0275	.0293	.0287	.0250	.0218	.0177
-1.0	.0210	.0239	.0269	.0329	.0417	.0471	.0516	.0546	.0520	.0486	.0436
-.8	.0346	.0385	.0425	.0509	.0642	.0735	.0827	.0937	.0957	.0938	.0890
-.6	.0518	.0568	.0620	.0732	.0927	.1077	.1244	.1507	.1651	.1690	.1689
-.4	.0719	.0781	.0847	.0994	.1267	.1496	.1773	.2294	.2699	.2898	.3068
-.2	.0939	.1016	.1106	.1287	.1672	.1980	.2418	.3296	.4147	.4684	.5280
0	.1189	.1276	.1372	.1600	.2066	.2500	.3086	.4444	.5917	.6944	.8264
.2	.1439	.1535	.1638	.1913	.2461	.3020	.3755	.5593	.7687	.9205	1.1249
.4	.1659	.1770	.1897	.2206	.2865	.3504	.4400	.6594	.9135	1.0991	1.3461
.6	.1860	.1983	.2124	.2468	.3206	.3923	.4929	.7382	1.0184	1.2199	1.4840
.8	.2032	.2166	.2318	.2691	.3490	.4265	.5346	.7952	1.0877	1.2951	1.5639
1.0	.2169	.2312	.2475	.2871	.3716	.4529	.5657	.8343	1.1314	1.3402	1.6093
1.2	.2273	.2424	.2595	.3010	.3887	.4725	.5880	.8601	1.1584	1.3671	1.6352
1.4	.2350	.2507	.2684	.3113	.4011	.4864	.6033	.8768	1.1749	1.3829	1.6499
1.6	.2403	.2565	.2747	.3186	.4098	.4960	.6134	.8872	1.1847	1.3920	1.6582
1.8	.2439	.2604	.2790	.3235	.4156	.5015	.6200	.8935	1.1903	1.3971	1.6627
2.0	.2452	.2619	.2807	.3255	.4180	.5049	.6227	.8960	1.1923	1.3988	1.6640

TABLE I.- BOUNDARY-INDUCED-UPWASH FACTOR F - Continued

(d) $\eta = 0.7$

ξ	F										
	$\sigma = -0.9$	$\sigma = -0.8$	$\sigma = -0.7$	$\sigma = -0.5$	$\sigma = -0.2$	$\sigma = 0$	$\sigma = 0.2$	$\sigma = 0.5$	$\sigma = 0.7$	$\sigma = 0.8$	$\sigma = 0.9$
-2.0	-0.0076	-0.0072	-0.0069	-0.0063	-0.0060	-0.0062	-0.0069	-0.0089	-0.0108	-0.0119	-0.0132
-1.8	-.0066	-.0060	-.0055	-.0047	-.0039	-.0040	-.0046	-.0069	-.0093	-.0109	-.0125
-1.6	-.0036	-.0027	-.0019	-.0004	.0012	.0016	.0013	-.0012	-.0045	-.0066	-.0090
-1.4	.0009	.0022	.0035	.0059	.0090	.0103	.0107	.0086	.0046	.0017	-.0017
-1.2	.0074	.0092	.0111	.0149	.0202	.0233	.0253	.0250	.0208	.0171	.0123
-1.0	.0160	.0187	.0213	.0269	.0358	.0419	.0474	.0520	.0495	.0456	.0393
-.8	.0272	.0308	.0345	.0425	.0567	.0677	.0794	.0957	.1004	.0984	.0920
-.6	.0411	.0457	.0507	.0620	.0834	.1018	.1243	.1651	.1911	.1993	.2001
-.4	.0572	.0630	.0695	.0847	.1157	.1447	.1836	.2699	.3501	.3941	.4329
-.2	.0766	[a].0821	[a].0903	.1106	.1526	.1951	.2566	.4147	[a].6114	[a].7602	.9397
0	.0941	.1027	.1126	.1372	.1924	.2500	.3380	.5917	.9612	1.2913	1.8262
.2	.1116	[a].1233	[a].1349	.1638	.2321	.3049	.4195	.7687	[a]1.3110	[a]1.8224	2.7126
.4	.1310	.1425	.1558	.1897	.2690	.3553	.4924	.9135	1.5722	2.1886	3.2194
.6	.1470	.1597	.1745	.2124	.3013	.3982	.5517	1.0184	1.7312	2.3833	3.4522
.8	.1609	.1747	.1908	.2318	.3280	.4323	.5966	1.0877	1.8219	2.4842	3.5603
1.0	.1721	.1868	.2039	.2475	.3489	.4581	.6287	1.1314	1.8728	2.5371	3.6130
1.2	.1808	.1962	.2141	.2595	.3645	.4767	.6507	1.1584	1.9015	2.5655	3.6400
1.4	.1872	.2032	.2217	.2684	.3758	.4897	.6654	1.1749	1.9177	2.5809	3.6540
1.6	.1918	.2082	.2271	.2747	.3835	.4984	.6748	1.1847	1.9268	2.5892	3.6613
1.8	.1948	.2115	.2307	.2790	.3887	.5040	.6807	1.1903	1.9317	2.5935	3.6648
2.0	.1958	.2127	.2321	.2807	.3907	.5062	.6829	1.1923	1.9331	2.5946	3.6655

[a]Values determined by Lagrange's interpolation formula because of slow convergence of equation (7).

TABLE I.- BOUNDARY-INDUCED-UPWASH FACTOR F - Concluded

(e) $\eta = 0.9$

ξ	F										
	$\sigma = -0.9$	$\sigma = -0.8$	$\sigma = -0.7$	$\sigma = -0.5$	$\sigma = -0.2$	$\sigma = 0$	$\sigma = 0.2$	$\sigma = 0.5$	$\sigma = 0.7$	$\sigma = 0.8$	$\sigma = 0.9$
-2.0	-0.0081	-0.0079	-0.0076	-0.0074	-0.0074	-0.0079	-0.0088	-0.0111	-0.0132	-0.0143	-0.0156
-1.8	-.0073	-.0069	-.0066	-.0061	-.0058	-.0062	-.0071	-.0098	-.0125	-.0141	-.0159
-1.6	-.0048	-.0042	-.0036	-.0025	-.0015	-.0015	-.0022	-.0053	-.0090	-.0113	-.0139
-1.4	-.0011	-.0001	.0009	.0028	.0051	.0060	.0059	.0029	-.0017	-.0050	-.0088
-1.2	.0043	.0058	.0074	.0105	.0150	.0176	.0192	.0177	.0123	.0079	.0023
-1.0	.0116	.0138	.0160	.0210	.0291	.0348	.0400	.0436	.0393	.0338	.0257
-.8	.0209	.0240	.0272	.0346	.0483	.0594	.0718	.0890	.0920	.0875	.0770
-.6	.0325	.0366	.0411	.0518	.0734	.0932	.1190	.1689	.2001	.2066	.1997
-.4	.0465	.0511	.0572	.0719	.1044	.1373	.1854	.3068	.4329	.5006	.5476
-.2	[a].0616	[a].0672	.0766	.0939	.1397	.1908	.2726	.5280	.9397	[a]1.4490	[a]2.5968
0	.0763	.0845	.0941	.1189	.1795	.2500	.3718	.8264	1.8262	3.1888	6.9252
.2	[a].0910	[a].1018	.1116	.1439	.2194	.3092	.4710	1.1249	2.7126	[a]4.9286	[a]11.2536
.4	.1061	.1179	.1310	.1659	.2547	.3627	.5582	1.3461	3.2194	5.8770	13.3028
.6	.1201	.1324	.1470	.1860	.2857	.4068	.6246	1.4840	3.4522	6.1710	13.6507
.8	.1317	.1451	.1609	.2032	.3108	.4406	.6718	1.5639	3.5603	6.2901	13.7734
1.0	.1411	.1553	.1721	.2169	.3300	.4652	.7036	1.6093	3.6130	6.3437	13.8247
1.2	.1483	.1632	.1808	.2273	.3441	.4824	.7244	1.6352	3.6400	6.3696	13.8482
1.4	.1537	.1691	.1872	.2350	.3539	.4940	.7377	1.6499	3.6540	6.3825	13.8592
1.6	.1575	.1732	.1918	.2403	.3606	.5015	.7458	1.6582	3.6613	6.3889	13.8643
1.8	.1600	.1760	.1948	.2439	.3649	.5062	.7507	1.6627	3.6648	6.3917	13.8663
2.0	.1608	.1769	.1958	.2452	.3665	.5079	.7524	1.6640	3.6655	6.3919	13.8660

[a]Values determined by Lagrange's interpolation formula because of slow convergence of equation (7).

TABLE II.- VALUES OF τ AT POINTS (ξ,η) DUE TO INFINITESIMAL LIFTING ELEMENTS LOCATED AT POINTS $(0,\pm\sigma)$

η	ξ	τ					
		$\sigma = 0$	$\sigma = 0.2$	$\sigma = 0.5$	$\sigma = 0.7$	$\sigma = 0.8$	$\sigma = 0.9$
0	0	0	0	0	0	0	0
	.2	.1971	.1996	.2081	.2195	.2272	.2370
	.4	.3831	.3861	.4014	.4211	.4344	.4508
	.6	.5466	.5502	.5691	.5926	.6083	.6271
	.8	.6828	.6865	.7059	.7293	.7445	.7624
	1.0	.7908	.7941	.8117	.8325	.8457	.8609
	1.2	.8724	.8753	.8900	.9070	.9176	.9296
	1.4	.9319	.9341	.9457	.9588	.9669	.9759
	1.6	.9734	.9751	.9838	.9936	.9995	1.0060
	1.8	1.0014	1.0026	1.0090	1.0159	1.0201	1.0247
	2.0	1.0135	1.0145	1.0195	1.0249	1.0281	1.0316
0.2	0	0	0	0	0	0	0
	.2	.1996	.2030	.2063	.2285	.2362	.2522
	.4	.3861	.3899	.4100	.4356	.4530	.4744
	.6	.5502	.5547	.5788	.6084	.6280	.6512
	.8	.6865	.6911	.7149	.7433	.7613	.7822
	1.0	.7941	.7982	.8191	.8431	.8580	.8747
	1.2	.8753	.8786	.8954	.9141	.9255	.9379
	1.4	.9341	.9366	.9493	.9630	.9711	.9799
	1.6	.9751	.9769	.9859	.9954	1.0009	1.0068
	1.8	1.0026	1.0038	1.0099	1.0161	1.0197	1.0234
	2.0	1.0145	1.0154	1.0198	1.0243	1.0268	1.0294
0.5	0	0	0	0	0	0	0
	.2	.2081	.2063	.2417	.2793	.3066	.3421
	.4	.4014	.4100	.4559	.5135	.5525	.5994
	.6	.5691	.5788	.6296	.6885	.7254	.7666
	.8	.7059	.7149	.7609	.8103	.8390	.8692
	1.0	.8117	.8191	.8553	.8918	.9117	.9317
	1.2	.8900	.8954	.9210	.9453	.9580	.9702
	1.4	.9457	.9493	.9655	.9801	.9873	.9939
	1.6	.9838	.9859	.9948	1.0022	1.0056	1.0083
	1.8	1.0090	1.0099	1.0134	1.0158	1.0165	1.0168
	2.0	1.0195	1.0198	1.0208	1.0208	1.0204	1.0195
0.7	0	0	0	0	0	0	0
	.2	.2195	.2285	.2793	.3466	.3957	.4707
	.4	.4211	.4356	.5135	.6092	.6721	.7448
	.6	.5926	.6084	.6885	.7748	.8242	.8744
	.8	.7293	.7433	.8103	.8744	.9073	.9379
	1.0	.8325	.8431	.8918	.9340	.9539	.9712
	1.2	.9070	.9141	.9453	.9703	.9811	.9897
	1.4	.9588	.9630	.9801	.9925	.9972	1.0004
	1.6	.9936	.9954	1.0022	1.0059	1.0067	1.0066
	1.8	1.0159	1.0161	1.0158	1.0139	1.0121	1.0100
	2.0	1.0249	1.0243	1.0208	1.0165	1.0138	1.0108
0.9	0	0	0	0	0	0	0
	.2	.2370	.2522	.3421	.4707	.5368	.6203
	.4	.4508	.4744	.5994	.7448	.8315	.9151
	.6	.6271	.6512	.7666	.8744	.9257	.9668
	.8	.7624	.7822	.8692	.9379	.9660	.9860
	1.0	.8609	.8747	.9317	.9712	.9855	.9947
	1.2	.9296	.9379	.9702	.9897	.9958	.9991
	1.4	.9759	.9799	.9939	1.0004	1.0015	1.0014
	1.6	1.0060	1.0068	1.0083	1.0066	1.0047	1.0027
	1.8	1.0247	1.0234	1.0168	1.0100	1.0064	1.0033
	2.0	1.0316	1.0294	1.0195	1.0108	1.0068	1.0034

TABLE III.- CONSTANTS USED IN COMPUTATIONS FOR ILLUSTRATIVE EXAMPLE

$\beta = 1.00$	$\tan \Lambda_{0.50} = \tan \Lambda_0 - \frac{c_s}{b}(1 - \lambda) = 0.9251$
$A = 5.11$	$\tan \Lambda_{0.75} = \tan \Lambda_{0.50} - \frac{c_s}{2b}(1 - \lambda) = 0.8377$
$A_t = 4.01$	$\tan(\Lambda_{0.75})_t = \tan 40^\circ = 0.8391$
$\lambda = 0.383$	$\frac{c_s}{2b} = 0.142$
$\lambda_t = 0.625$	$\frac{b}{2c'} = 2.396$
$\eta_{max} = \frac{b}{2r} = 0.656$	$\frac{x_0}{c'} = 1.095$
$(\eta_{max})_t = \frac{b_t}{2r} = 0.239$	$\frac{c_s}{2r} = 0.186$
$a \approx 0.0587$ (from equation (54))	$\frac{l_s}{r} = 0.787$
$a' \approx 0.0544$ (from equation (55))	$\frac{dC_m}{di_t} = 0.0188$
$\tan \Lambda_0 = 1.0999$	$\frac{S}{4\pi r^2} = 0.0268$
$\tan \Lambda_{0.25} = \tan \Lambda_0 - \frac{c_s}{2b}(1 - \lambda) = 1.0125$	

TABLE IV.- DETERMINATION OF INDUCED-UPWASH FACTOR FOR ILLUSTRATIVE EXAMPLE

[β = 1.0; values of F obtained from figure 2]

$\frac{2s}{b}$	σ, $\frac{2s}{b}\frac{b}{2r}$	η = 0		η = 0.2		η = 0.5		η = 0.7		η = 0.9	
		ξ (1)	F	ξ (1)	F	ξ (1)	F	ξ (1)	F	ξ (1)	F
$F_{0.25}$ [$\tan \Lambda_{0.25} = 1.0125$]											
0.9239	0.606	-0.614	0.102	-0.411	0.177	-0.107	0.435	0.095	0.870		
.7071	.464	-.470	.135	-.267	.215	.036	.440	.239	.730		
.3827	.251	-.254	.187	-.052	.262	.252	.420	.455	.560		
0	0	0	.250	.203	.300	.506	.372	.709	.418		
-.3827	-.251	-.254	.187	-.052	.214	.252	.244	.455	.259		
-.7071	-.464	-.470	.135	-.267	.155	.036	.171	.239	.175		
-.9239	-.606	-.614	.102	-.411	.118	-.107	.132	.095	.134		
$F_{0.75}$ [$\frac{c_s}{2r} = 0.186$; $\tan \Lambda_{0.75} = 0.8377$]											
0.9239	0.606	-0.428	0.145	-0.260	0.227	-0.009	0.510	0.159	0.950		
.7071	.464	-.284	.178	.116	.265	.135	.500	.302	.790		
.3827	.251	-.068	.235	.099	.305	.351	.455	.518	.580		
0	0	.186	.295	.353	.335	.605	.392	.772	.425		
-.3827	-.251	-.068	.235	.099	.248	.351	.263	.518	.268		
-.7071	-.464	-.284	.178	-.116	.185	.135	.187	.302	.184		
-.9239	-.606	-.428	.145	-.262	.147	-.009	.146	.159	.142		
F_t [$\frac{l_s}{r} = 0.787$; $\tan(\Lambda_{0.75})_t = 0.8391$]											
0.9239	0.606	0.173	0.297	0.341	0.447	0.593	0.860				
.7071	.464	.317	.330	.485	.454	.737	.738				
.3827	.251	.533	.375	.701	.454	.953	.594				
0	0	.787	.418	.955	.443	1.207	.469				
-.3827	-.251	.533	.375	.701	.367	.953	.349				
-.7071	-.464	.317	.330	.485	.305	.737	.270				
-.9239	-.606	.173	.297	.341	.266	.593	.226				

(1) For $F_{0.25}$, $\xi = \frac{1}{\beta}\left[(\eta - |\sigma|)\tan \Lambda_{0.25}\right]$;

for $F_{0.75}$, $\xi = \frac{1}{\beta}\left(\frac{c_s}{2r} + \eta \tan \Lambda_{0.75} - |\sigma| \tan \Lambda_{0.25}\right)$;

for F_t, $\xi = \frac{1}{\beta}\left[\frac{l_s}{r} + \eta \tan(\Lambda_{0.75})_t - |\sigma| \tan \Lambda_{0.25}\right]$.

TABLE V.- CALCULATION OF INDUCED-ANGLE DISTRIBUTION ALONG ONE-QUARTER-CHORD LINE OF WING

FOR ILLUSTRATIVE EXAMPLE, SYMMETRICAL LIFT DISTRIBUTION (EQUATION (26a))

$$\left[\frac{S}{4\pi r^2} = 0.0268;\ \eta_{max} = 0.656\right]$$

①	②	③	④	⑤	⑥	⑦	⑧	⑨	⑩	⑪	⑫	⑬	⑭
2s/b	σ	$F_{+\sigma} + F_{-\sigma}$ (table IV)					$\frac{c_l c}{c_L \bar{c}}$ (fig. 6)	⑧ × ③	⑧ × ④	⑧ × ⑤	⑧ × ⑥	⑧ × ⑦	Multiplier
		η = 0	η = 0.2	η = 0.5	η = 0.7	η = 0.9		η = 0	η = 0.2	η = 0.5	η = 0.7	η = 0.9	
0.9239	0.606	0.204	0.295	0.567	1.004		0.607	0.1238	0.1791	0.3442	0.6094		0.20037
.7071	.464	.270	.370	.611	.905		.974	.2630	.3604	.5951	.8815		.18512
.3827	.251	.374	.476	.664	.819		1.143	.4275	.5441	.7590	.9361		.48374
0	0	.500	.600	.744	.836		1.111	.5555	.6666	.8266	.9288		.13090

NACA

η	$\left(\sum_{\text{to}}^{Q} ⑭ \times ⑨ \ \text{to}\ \sum ⑭ \times ⑬\right)$	$\left(\frac{w}{VC_L}\right)_{0.25}$ $\left(Q\frac{S}{4\pi r^2}\right)$	η/η_{max}
0	0.3530	0.0095	0
.2	.4531	.0121	.305
.5	.6545	.0175	.762
.7	.8597	.0230	1.067
.9			

Plot $\left(\frac{w}{VC_L}\right)_{0.25}$ against η/η_{max}.

TABLE VI.- CALCULATION OF INDUCED-ANGLE DISTRIBUTION ALONG THREE-QUARTER-CHORD LINE OF WING

FOR ILLUSTRATIVE EXAMPLE, SYMMETRICAL LIFT DISTRIBUTION (EQUATION (26a))

$$\left[\frac{S}{4\pi r^2} = 0.0268;\ \eta_{max} = 0.656\right]$$

①	②	③	④	⑤	⑥	⑦	⑧	⑨	⑩	⑪	⑫	⑬	⑭
2s/b	σ	$F_{+\sigma} + F_{-\sigma}$ (table IV)					$\frac{c_l c}{C_L \bar{c}}$ (fig. 6)	⑧ × ③	⑧ × ④	⑧ × ⑤	⑧ × ⑥	⑧ × ⑦	Multiplier
		η = 0	η = 0.2	η = 0.5	η = 0.7	η = 0.9		η = 0	η = 0.2	η = 0.5	η = 0.7	η = 0.9	
0.9239	0.606	0.290	0.374	0.656	1.092		0.607	0.1760	0.2270	0.3982	0.6628		0.20037
.7071	.464	.356	.450	.687	.974		.974	.3467	.4383	.6691	.9487		.18512
.3827	.251	.470	.553	.718	.848		1.143	.5372	.6321	.8207	.9693		.48374
0	0	.590	.670	.784	.850		1.111	.6555	.7444	.8710	.9444		.13090

NACA

η	$\left(\sum_{\text{to}}^{\text{to}} ⑭ \times ⑨ \Big/ \sum ⑭ \times ⑬\right)$	$\left(\frac{w}{VC_L}\right)_{0.75} \Big/ \left(q\frac{S}{4\pi r^2}\right)$	η/η_{max}
0	0.4451	0.0119	0
.2	.5298	.0142	.305
.5	.7147	.0192	.762
.7	.9009	.0241	1.067
.9			

Plot $\left(\frac{w}{VC_L}\right)_{0.75}$ against η/η_{max}.

TABLE VII.- CALCULATION OF INDUCED-ANGLE DISTRIBUTION ALONG THREE-QUARTER-CHORD LINE OF TAIL, SYMMETRICAL LIFT DISTRIBUTION (EQUATION (26a))

$\left[\frac{S}{4\pi r^2} = 0.0268;\ \eta_{max_t} = 0.239\right]$

①	②	③	④	⑤	⑥	⑦	⑧	⑨	⑩	⑪	⑫	⑬	⑭
2s/b	σ	$F_{+\sigma} + F_{-\sigma}$ (table IV)					$\frac{c_l c}{C_L \bar{c}}$ (fig. 6)	⑧ × ③	⑧ × ④	⑧ × ⑤	⑧ × ⑥	⑧ × ⑦	Multi-plier
		η = 0	η = 0.2	η = 0.5	η = 0.7	η = 0.9		η = 0	η = 0.2	η = 0.5	η = 0.7	η = 0.9	
0.9239	0.606	0.594	0.713	1.086			0.607	0.3606	0.4328	0.6592			0.20037
.7071	.464	.660	.759	1.008			.974	.6428	.7393	.9818			.18512
.3827	.251	.750	.821	.943			1.143	.8573	.9384	1.0778			.48374
0	0	.836	.886	.938			1.111	.9288	.9843	1.0421			.13090

NACA

η	$\left(\sum_{\text{to}}^{Q} ⑭ \times ⑨ \Big/ \sum ⑭ \times ⑬\right)$	$\left(\frac{w}{VC_L}\right)_t \Big/ \left(Q \frac{S}{4\pi r^2}\right)$	η/η_{max_t}
0	0.7275	0.0195	0
.2	.8064	.0216	.837
.5	.9716	.0260	2.092
.7			
.9			

Plot $\left(\frac{w}{VC_L}\right)_t$ against η/η_{max}.

TABLE VIII.- CALCULATION OF INDUCED-ANGLE DISTRIBUTION ALONG ONE-QUARTER-CHORD LINE OF WING, ANTISYMMETRICAL LIFT DISTRIBUTION (EQUATION (27))

$\left[\frac{S}{4\pi r^2} = 0.0268;\ \eta_{max} = 0.656\right]$

①	②	③	④	⑤	⑥	⑦	⑧	⑨	⑩	⑪	⑫	⑬	⑭
2s/b	σ	$F_{+\sigma} - F_{-\sigma}$ (table IV)					$\frac{c_l c}{C_l \bar{c}}$ (method of reference 10)	⑧ × ③ $\eta = 0$	⑧ × ④ $\eta = 0.2$	⑧ × ⑤ $\eta = 0.5$	⑧ × ⑥ $\eta = 0.7$	⑧ × ⑦ $\eta = 0.9$	Multiplier
		$\eta = 0$	$\eta = 0.2$	$\eta = 0.5$	$\eta = 0.7$	$\eta = 0.9$							
0.9239	0.606	0	0.059	0.303	0.736		5.522	0	0.3258	1.6732	4.0642		0.20037
.7071	.464	0	.060	.269	.555		6.362	0	.3817	1.7114	3.5309		.18512
.3827	.251	0	.048	.176	.301		.783	0	.0376	.1378	.2357		.48374
0	0	0	0	0	0		0	0	0	0	0		.13090

NACA

η	$\left(\sum_{\text{⑭ to ⑭}}^{Q} ⑭ \times ⑨ \Big/ \sum ⑭ \times ⑬\right)$	$\left(\frac{W}{VC_l}\right)_{0.25} \Big/ \left(Q\frac{S}{4\pi r^2}\right)$	η/η_{max}
0	0	0	0
.2	.1541	.0041	.305
.5	.7187	.0193	.762
.7	1.5820	.0424	1.067
.9			

Plot $\left(\frac{W}{VC_l}\right)_{0.25}$ against η/η_{max}.

TABLE IX.- CALCULATION OF INDUCED-ANGLE DISTRIBUTION ALONG THREE-QUARTER-CHORD LINE OF WING, ANTISYMMETRICAL LIFT DISTRIBUTION (EQUATION (27))

$\left[\frac{S}{4\pi r^2} = 0.0268;\ \eta_{max} = 0.656\right]$

①	②	③	④	⑤	⑥	⑦	⑧	⑨	⑩	⑪	⑫	⑬	⑭
2s/b	σ	$F_{+\sigma} - F_{-\sigma}$ (table IV)					$\frac{c_l c}{C_l \bar{c}}$ (method of reference 10)	⑧ × ③ η = 0	⑧ × ④ η = 0.2	⑧ × ⑤ η = 0.5	⑧ × ⑥ η = 0.7	⑧ × ⑦ η = 0.9	Multiplier
		η = 0	η = 0.2	η = 0.3	η = 0.7	η = 0.9							
0.9239	0.606	0	0.080	0.364	0.808		5.522	0	0.4418	2.0100	4.4618		0.20037
.7071	.464	0	.080	.313	.606		6.362	0	.5090	1.9913	3.8554		.18512
.3827	.251	0	.057	.192	.312		.783	0	.0446	.1503	.2443		.48374
0	0	0	0	0	0		0	0	0	0	0		.13090

NACA

η	$\left(\sum_{\text{to}}^{Q} ⑭ \times ⑨ \Big/ \sum ⑭ \times ⑬\right)$	$\left(\frac{W}{VC_l}\right)_{0.75}\Big/\left(Q\frac{S}{4\pi r^2}\right)$	η/η_{max}
0	0	0	0
.2	.2043	.0055	.305
.5	.8441	.0226	.762
.7	1.7259	.0463	1.067
.9			

Plot $\left(\frac{W}{VC_l}\right)_{0.75}$ against η/η_{max}.

TABLE X.- JET-BOUNDARY CORRECTIONS FOR ANGLE OF ATTACK AND DRAG

(EQUATIONS (29) AND (30))

①	②	③	④	⑤	⑥	⑦
2y/b	$\frac{c_l c}{C_L \bar{c}}$ (fig. 6)	$\left(\frac{w}{VC_L}\right)_{0.25}$ (fig. 7)	$\left(\frac{w}{VC_L}\right)_{0.75}$ (fig. 7)	② × ③	② × ④	Multipliers
0	1.111	0.0095	0.0119	0.0106	0.0132	0.13090
.3827	1.143	.0128	.0149	.0146	.0170	.48374
.7071	.974	.0166	.0182	.0162	.0177	.18512
.9239	.607	.0201	.0214	.0122	.0130	.20037

$$\Delta\alpha_j = 57.3 \left[\sum ⑥ \times ⑦\right] C_L = 57.3\ (0.0158) C_L = 0.905 C_L$$

$$\Delta C_{D_j} = \left[\sum ⑤ \times ⑦\right] C_L^2 = 0.0139 C_L^2$$

TABLE XI.- JET-BOUNDARY CORRECTION FOR WING PITCHING-MOMENT COEFFICIENT

(EQUATION (36))

①	②	③	④	⑤	⑥	⑦	⑧	⑨
$\frac{2y}{b}$	$\frac{c_l c}{C_L \bar{c}}$ (fig. 6)	$\frac{c^2}{\bar{c}c'}$	④ (table X)	④ - ③ (table X)	② × ④	③ × ⑤	Area multiplier	Moment multiplier
0	1.111	1.961183	0.0119	0.0024	0.0132	0.00471	0.13090	0
.3827	1.143	1.144357	.0149	.0021	.0170	.00240	.48374	.18512
.7071	.974	.623224	.0182	.0016	.0177	.00100	.18512	.13090
.9239	.607	.362545	.0214	.0013	.0130	.00047	.20037	.18512

$$\frac{\Delta C_{L_1}}{57.3aC_L} = \sum ⑥ \times ⑧ = 0.01585$$

$$\frac{2y_1}{b} = K_2 \sum ② \times ⑨ + K_1 \frac{\sum ⑥ \times ⑨}{\sum ⑥ \times ⑧} = 0.48349$$

$$\frac{x_1}{c'} = \frac{2y_1}{b} \frac{b}{2c'} \tan \Lambda_{0.25} = 1.173$$

$$\Delta C_{m_1} = \frac{\Delta C_{L_1}}{57.3aC_L} \left(\frac{x_1 - x_0}{c'} \right) 57.3aC_L = 0.004C_L$$

$$\Delta C_{m_2} = \frac{\pi}{4} \cos \Lambda_{0.50} C_L \sum ⑦ \times ⑧ = 0.001C_L$$

$$\Delta C_{m_j} = 0.005C_L$$

$$\frac{c^2}{\bar{c}c'} = 3 \frac{\left[1 - (1 - \lambda) \frac{2y}{b} \right]^2}{\lambda^2 + \lambda + 1}$$

$a \approx 0.0587$

$$K_1 = \frac{1}{1 + \frac{36.48a}{A}} = 0.70469$$

$$K_2 = \frac{\frac{36.48a}{A}}{1 + \frac{36.48a}{A}} = 0.29531$$

TABLE XII.- JET-BOUNDARY CORRECTION TO DOWNWASH ANGLE AND ADDITIONAL JET-BOUNDARY CORRECTION FOR PITCHING-MOMENT COEFFICIENT FOR WING-PLUS-TAIL CONFIGURATION

(EQUATIONS (37) and (40))

$\left[\frac{V}{V_t} \text{ is assumed equal to } 1\right]$

①	②	③	④	⑤
2y/b	$\left(\frac{c_l c}{C_L \bar{c}}\right)_t$ (fig. 6)	$\left(\frac{w}{VC_L}\right)_t$ (fig. 7)	② × ③	Multipliers
0	1.104	0.0195	0.0215	0.13090
.3827	1.143	.0203	.0232	.48374
.7071	.989	.0211	.0209	.18512
.9239	.597	.0218	.0130	.20037

$$\Delta\epsilon_t = 57.3\left[\sum ④ \times ⑤\right]C_L = 1.175C_L$$

$$\Delta\alpha_j = 0.905C_L \quad \text{(from table X)}$$

$$\Delta\alpha_t = \Delta\epsilon_t - \Delta\alpha_j = 0.270C_L$$

$$\Delta C_{m_t} = \Delta\alpha_t \frac{dC_m}{di_t} = 0.005C_L$$

TABLE XIII.- ROLLING-MOMENT AND YAWING-MOMENT CORRECTIONS

(EQUATIONS (42) AND (48))

①	②	③	④	⑤	⑥	⑦	⑧	⑨	⑩
2y/b	$\frac{c_l c}{C_L \bar{c}}$ (fig. 6)	$\frac{c_l c}{C_l \bar{c}}$ (method of reference 10)	$\left(\frac{w}{VC_L}\right)_{0.25}$ (fig. 8)	$\left(\frac{w}{VC_l}\right)_{0.25}$ (fig. 8)	$\left(\frac{w}{VC_l}\right)_{0.75}$	⑥ × ②	⑤ × ②	④ × ③	Multi-plier
0	1.111	0	0.0094	0	0	0	0	0	0
.3827	1.143	.783	.0128	.0058	.0075	.00857	.00663	.01002	.09256
.7071	.974	6.362	.0166	.0167	.0198	.01929	.01627	.10561	.06545
.9239	.607	5.522	.0201	.0282	.0321	.01948	.01712	.11099	.09256

$$\Delta C_{l_j} = - C_{l_u} 57.3 a' \left[K_1 \times \sum ⑦ \times ⑩ \right] = -0.01007 C_{l_u}$$

$$a' = 0.0544$$

$$K_1 = \frac{1}{1 + \frac{18.24 a'}{A}} = 0.83739$$

$$C_l = C_{l_u} \left(1 + \frac{\Delta C_{l_j}}{C_{l_u}} \right) = 0.98993 C_{l_u}$$

$$\Delta C_{n_2} = - C_L C_{l_u} \left[\sum ⑧ \times ⑩ \right] = -0.00326 C_L C_{l_u}$$

$$\Delta C_{n_3} = - C_L C_{l_u} \left[\sum ⑨ \times ⑩ \right] = -0.01811 C_L C_{l_u}$$

$$\Delta C_n = \Delta C_{n_2} + \Delta C_{n_3} = -0.02137 C_L C_{l_u} = -.02159 C_L C_l$$

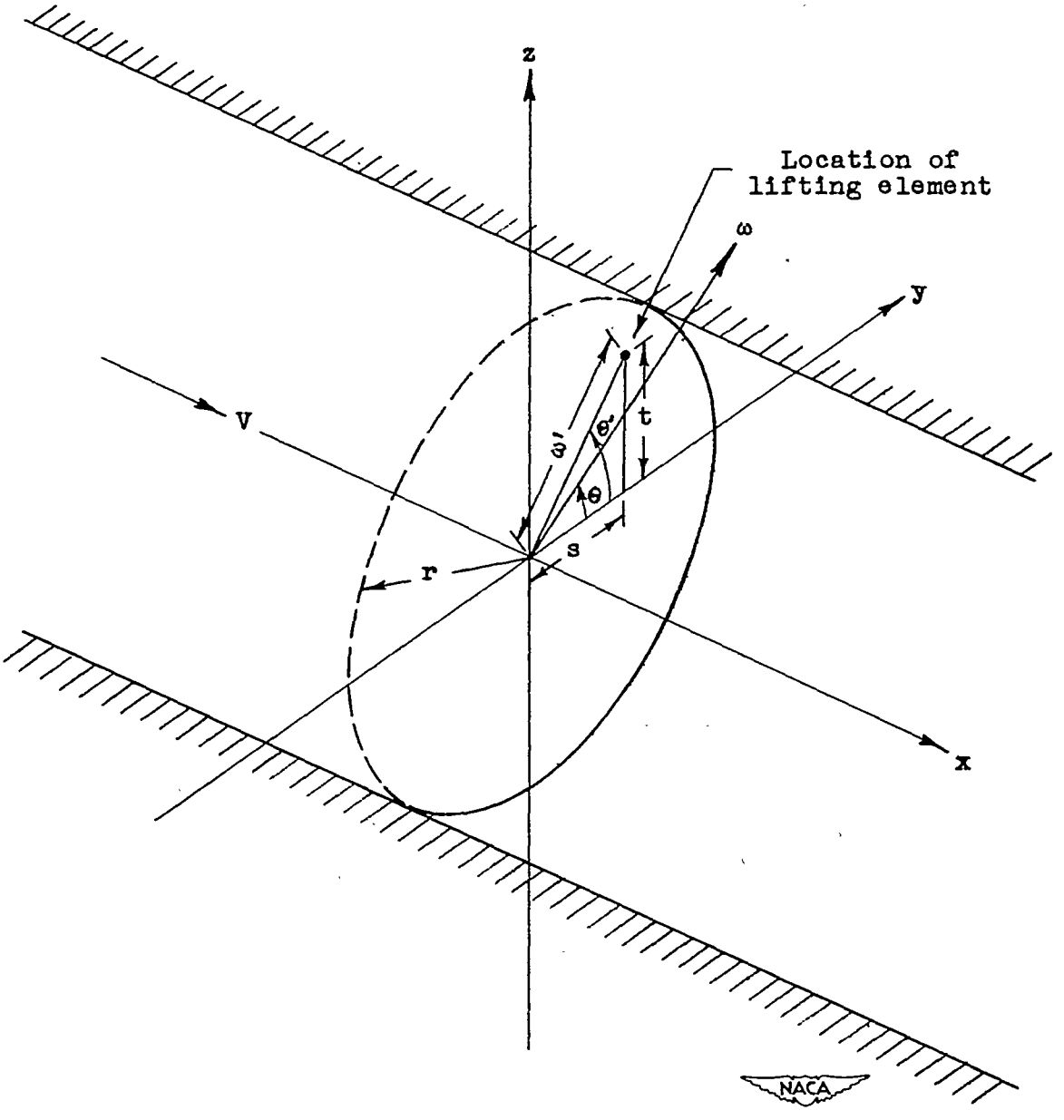

Figure 1.- Coordinate systems in closed circular wind tunnel.

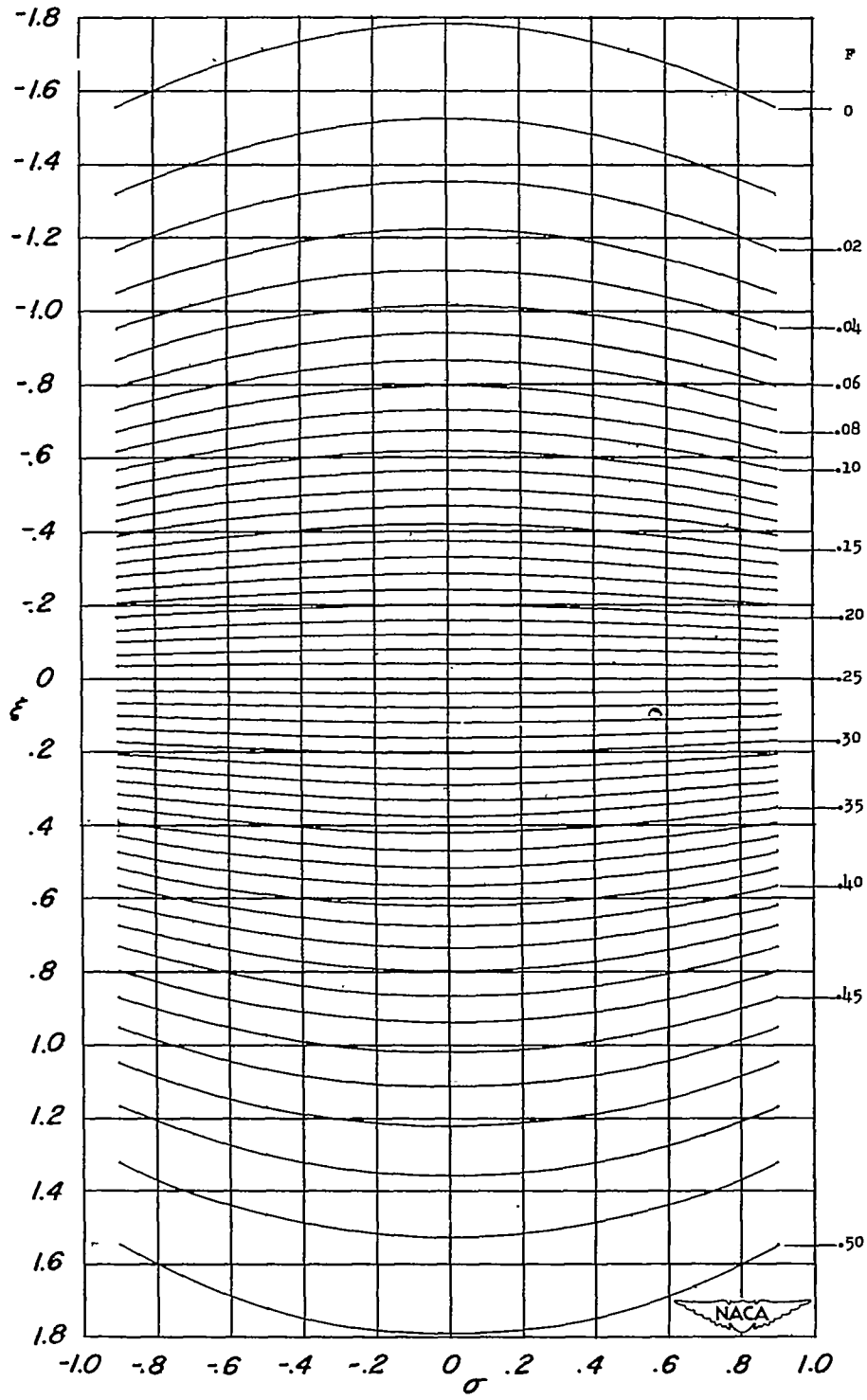

(a) $\eta = 0$.

Figure 2.- Contours of constant values of jet-boundary-induced-upwash factor F for a closed circular wind tunnel.

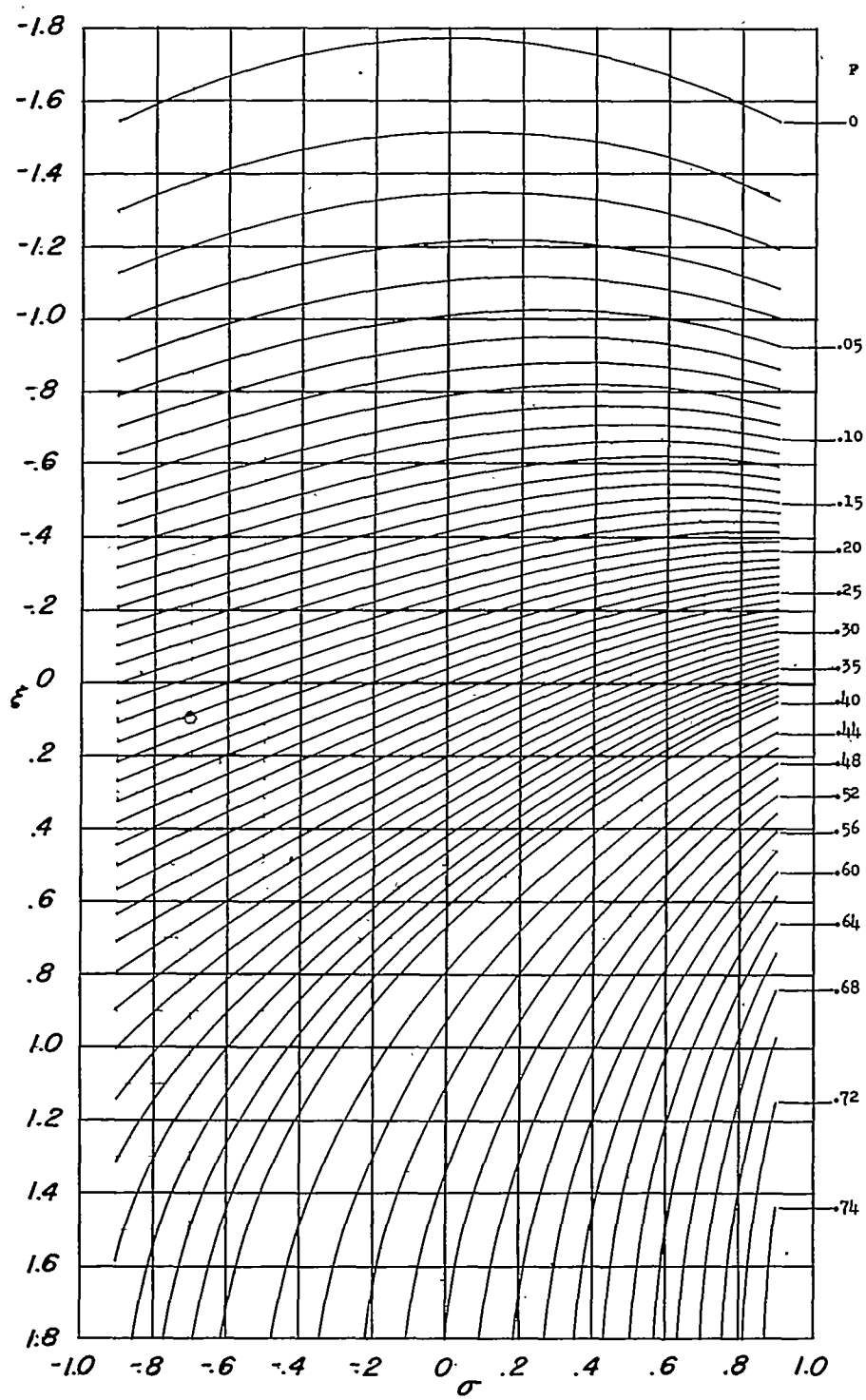

(b) $\eta = 0.2$.

Figure 2.- Continued.

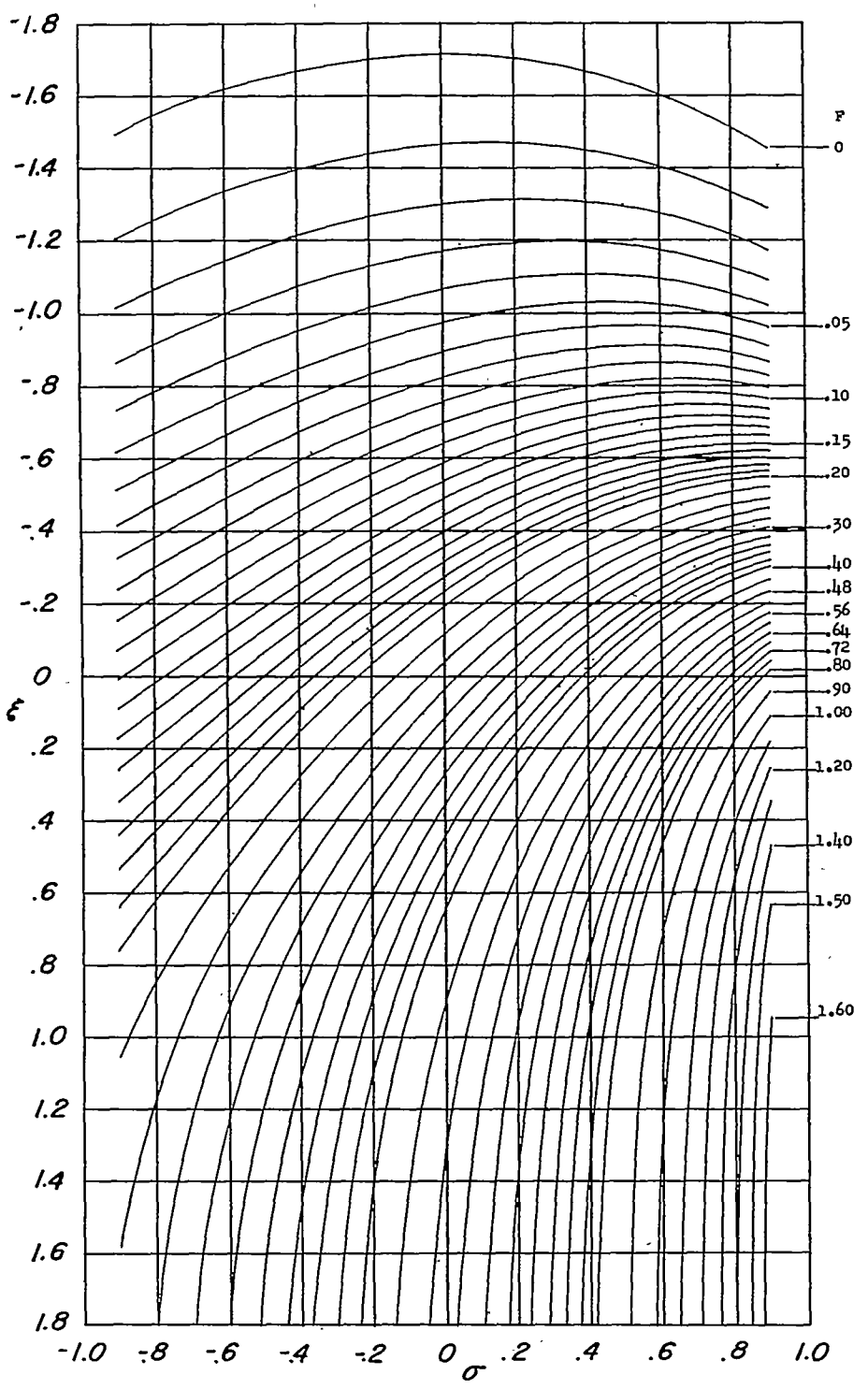

(c) $\eta = 0.5$.

Figure 2.- Continued.

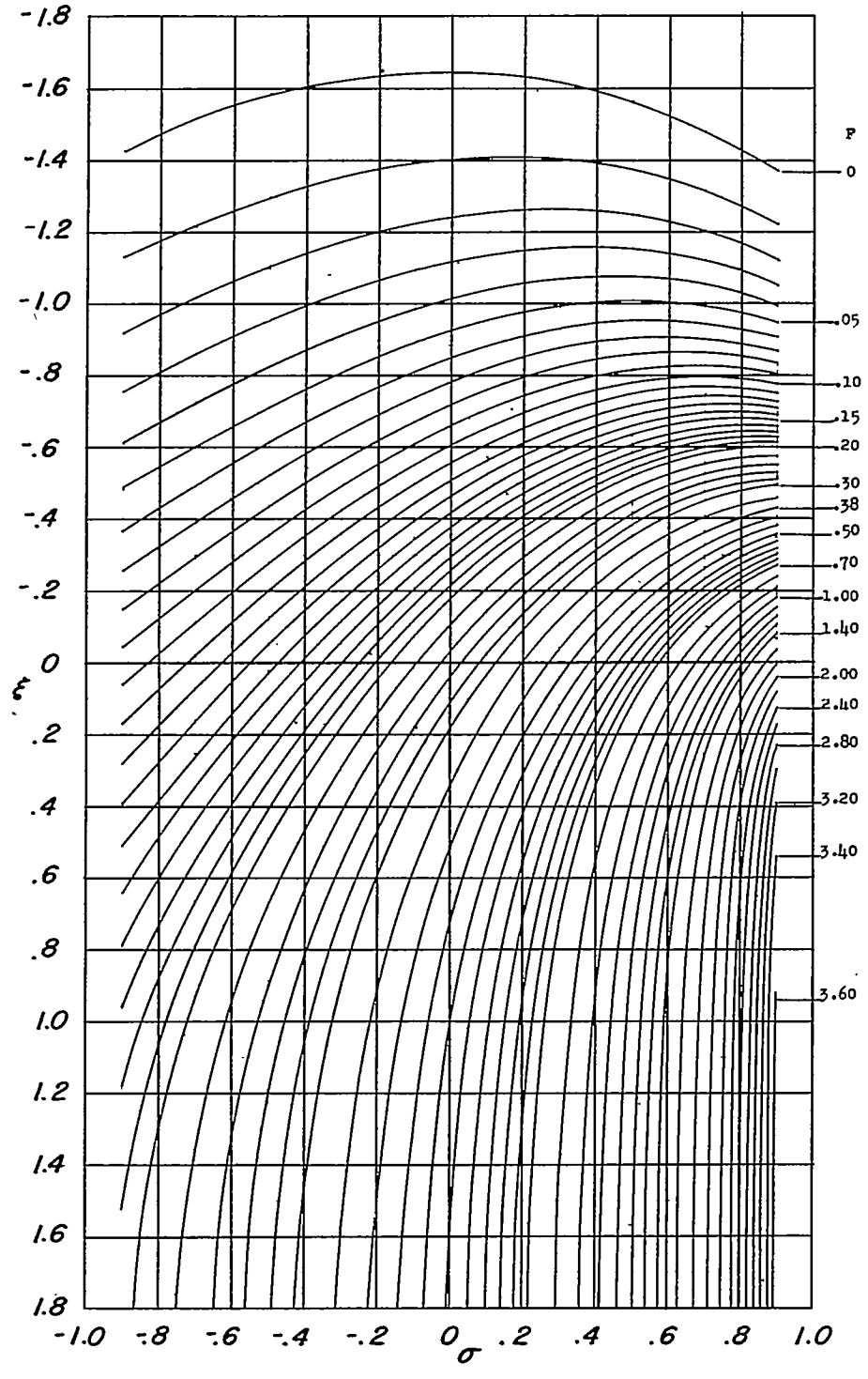

(d) $\eta = 0.7$.

Figure 2.- Continued.

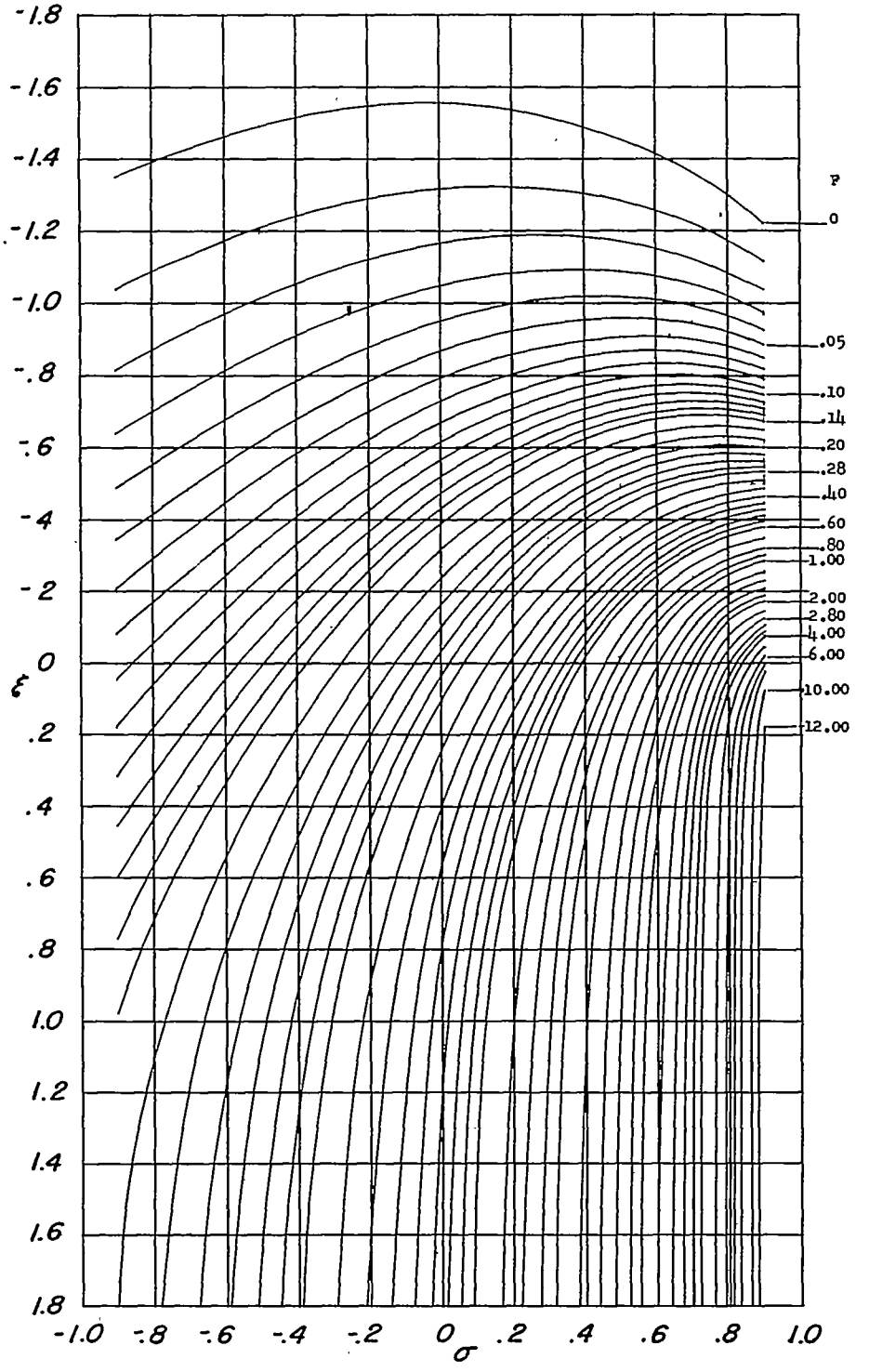

(e) $\eta = 0.9$.

Figure 2.- Concluded.

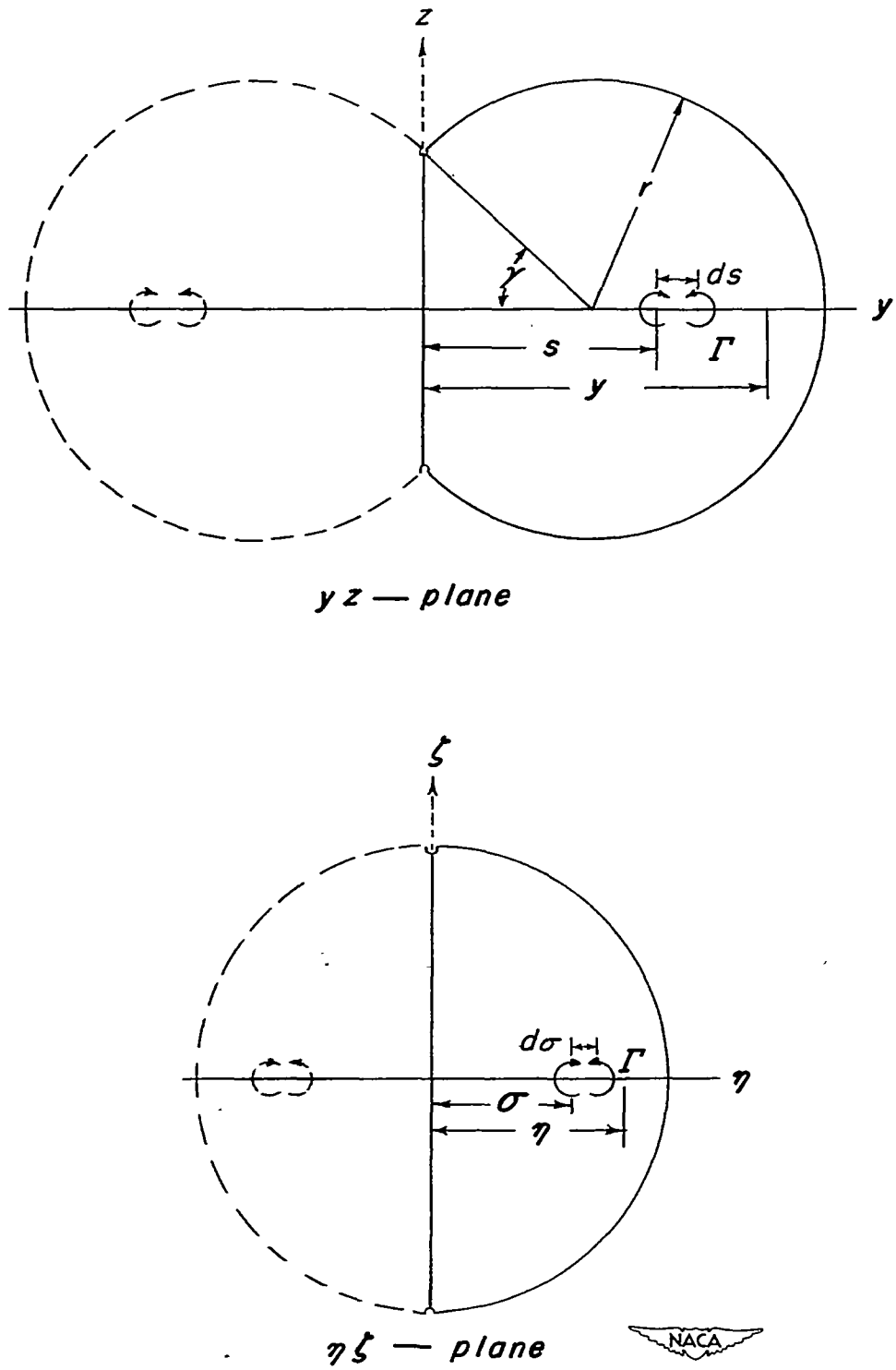

Figure 3.- Diagram of the bipolar tunnel including the reflected half of the jet and the circular jet into which the bipolar tunnel is transformed.

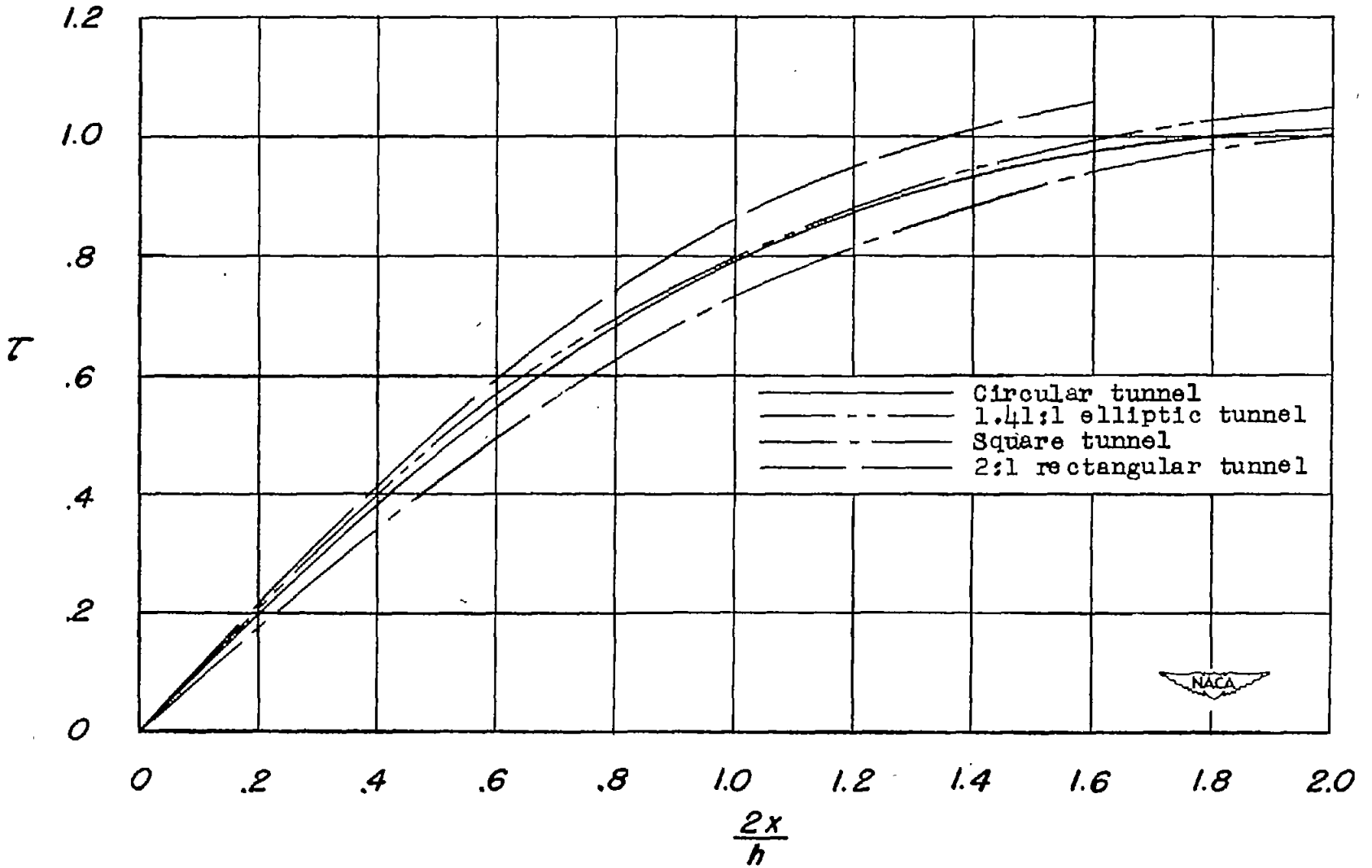

Figure 4.- Variation of τ along longitudinal center lines of several shapes of closed wind tunnels for infinitesimal lifting element located at the centers of the tunnels.

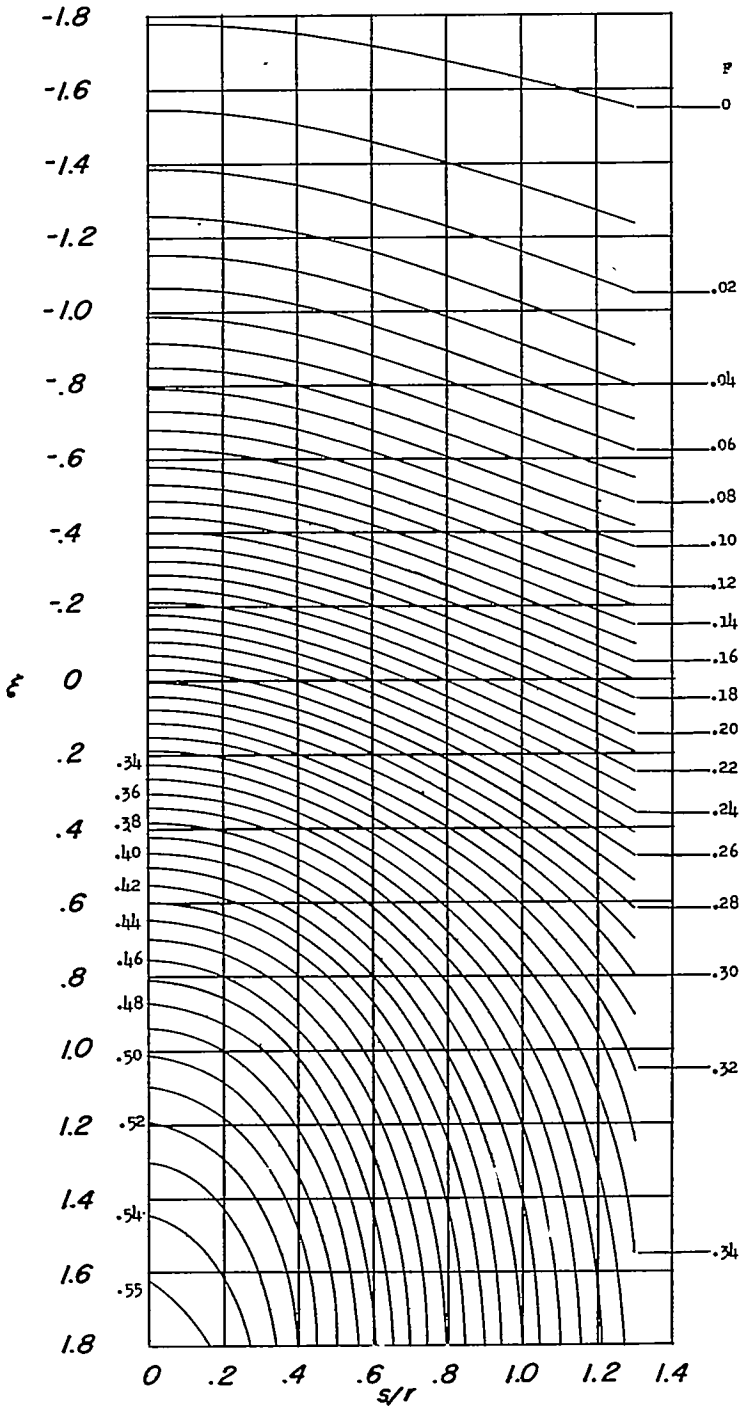

(a) $\frac{y}{r} = 0.$

Figure 5.- Contours of constant values of jet-boundary-induced-upwash factor F for a closed circular wind tunnel with reflection plane located 0.49781r from center line.

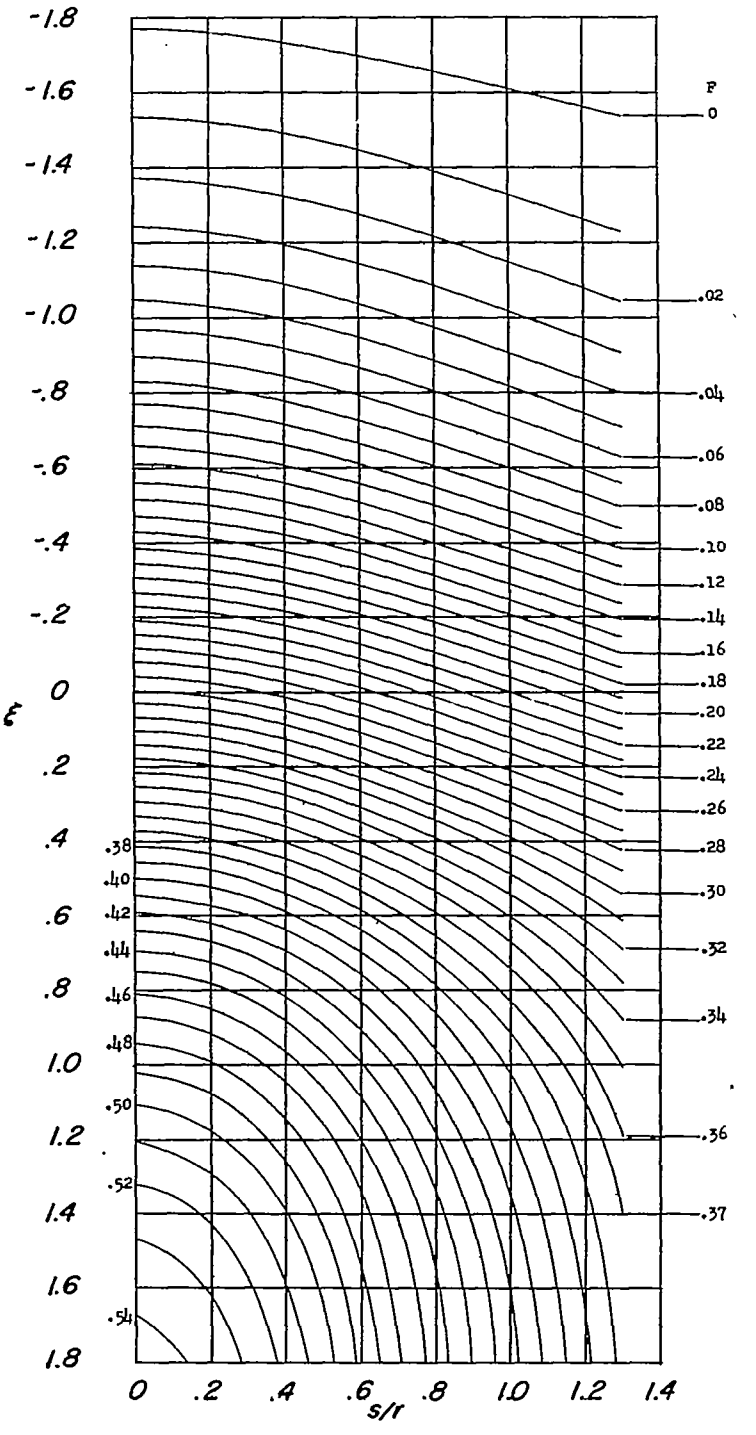

(b) $\frac{Y}{r} = 0.233$.

Figure 5.- Continued.

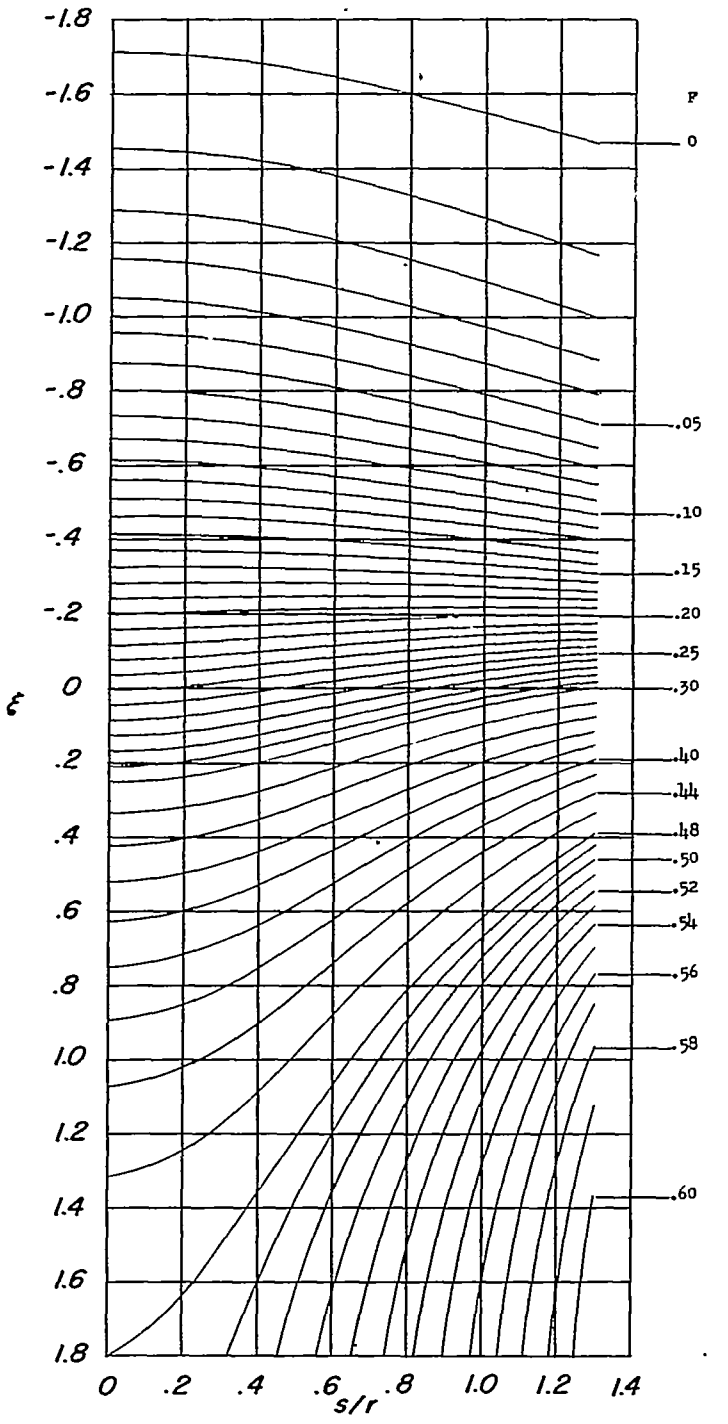

(c) $\frac{y}{r} = 0.616$.

Figure 5.- Continued.

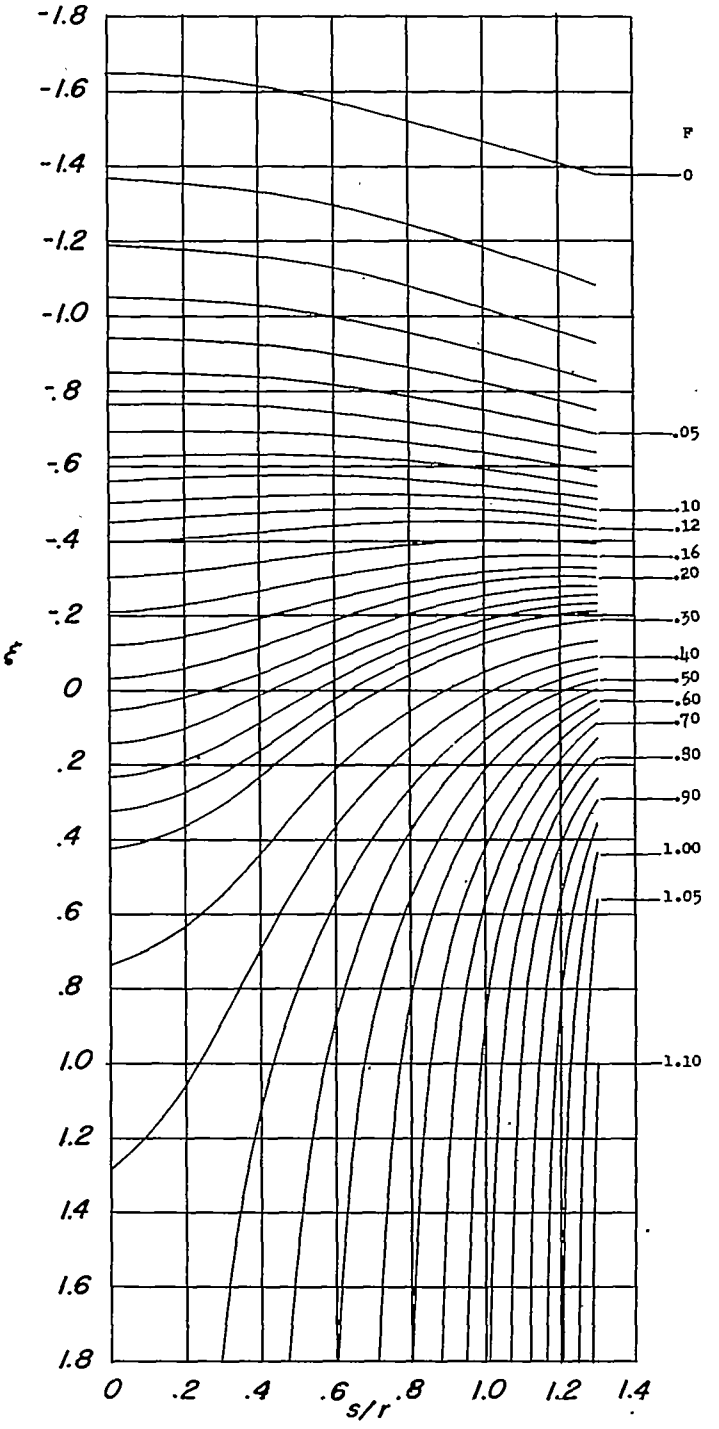

(d) $\frac{Y}{r} = 0.917$.

Figure 5.- Continued.

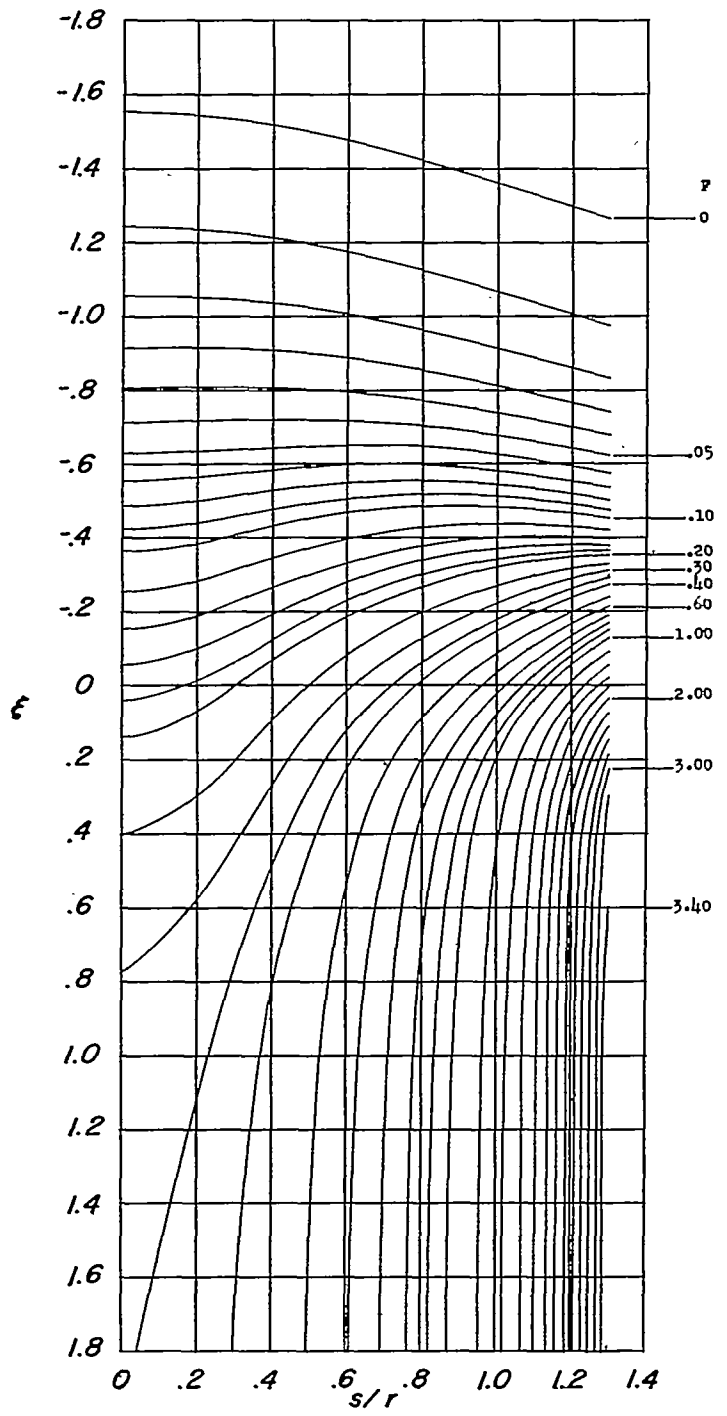

(e) $\frac{y}{r} = 1.282$.

Figure 5.- Concluded.

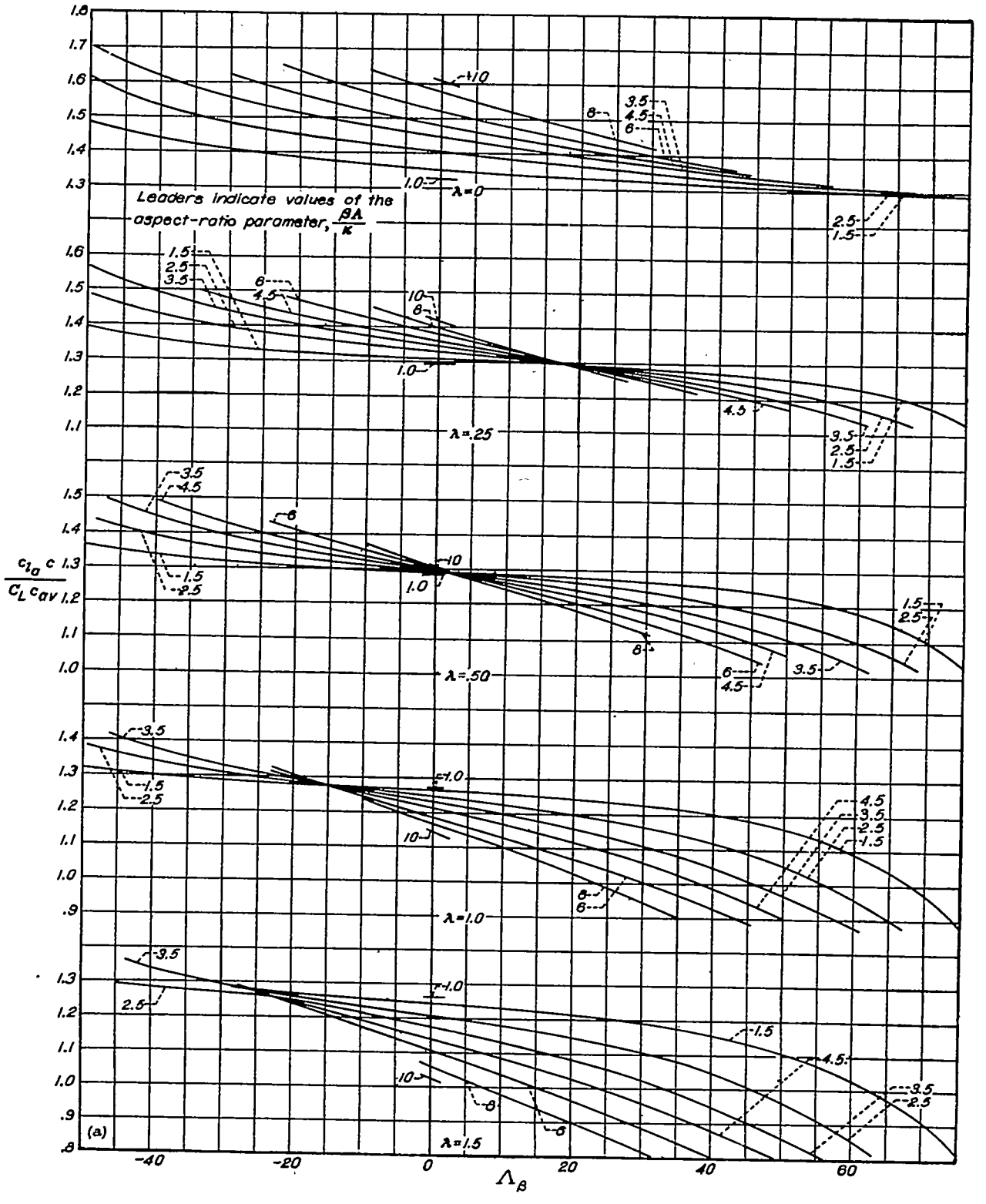

(a) Fraction of semispan, $\frac{2y}{b} = 0$.

Figure 6.- Variation of spanwise loading coefficient with sweep for various aspect ratios and taper ratios.

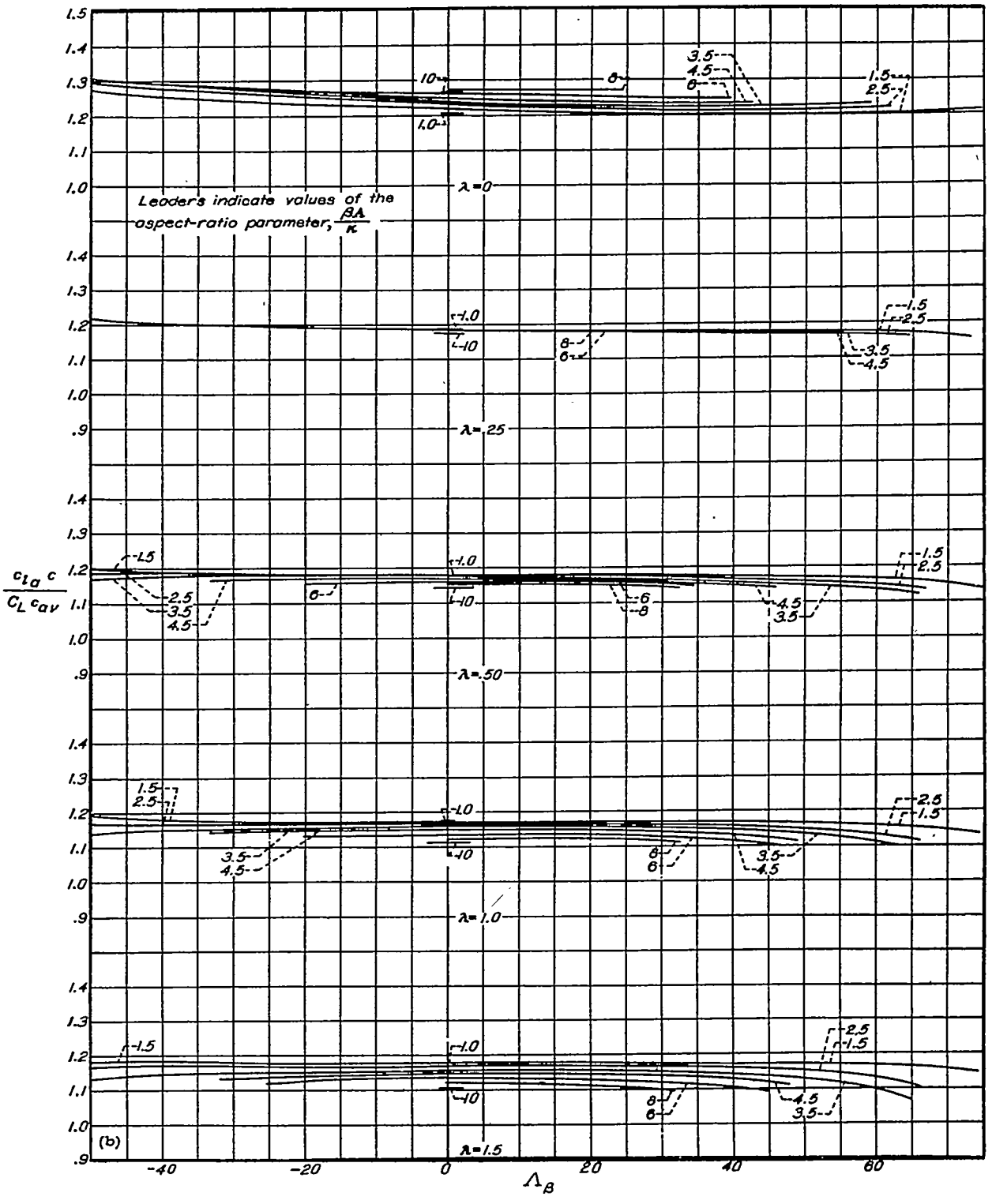

(b) Fraction of semispan, $\frac{2y}{b} = 0.3827$.

Figure 6.- Continued.

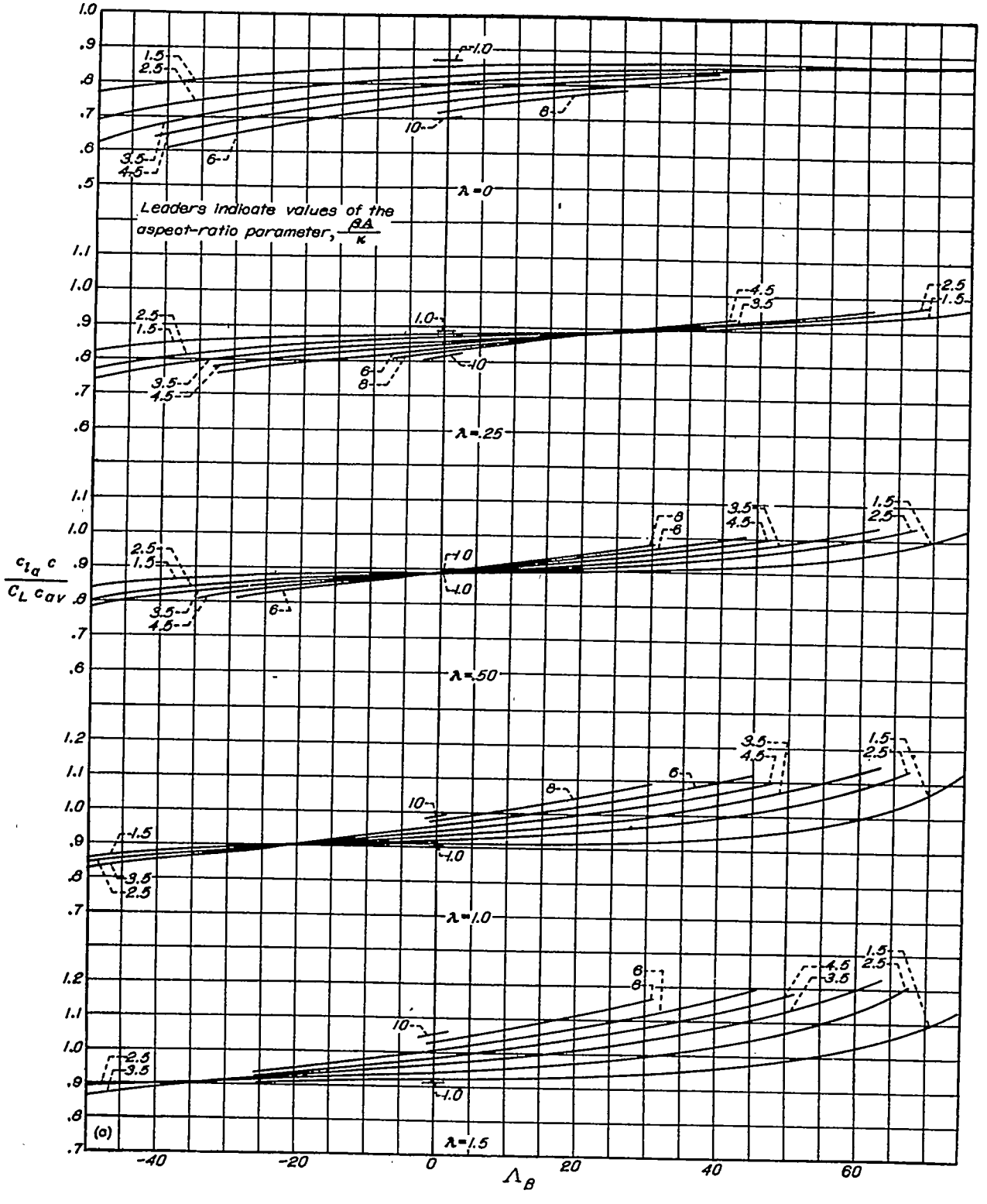

(c) Fraction of semispan, $\frac{2y}{b} = 0.7071$.

Figure 6.- Continued.

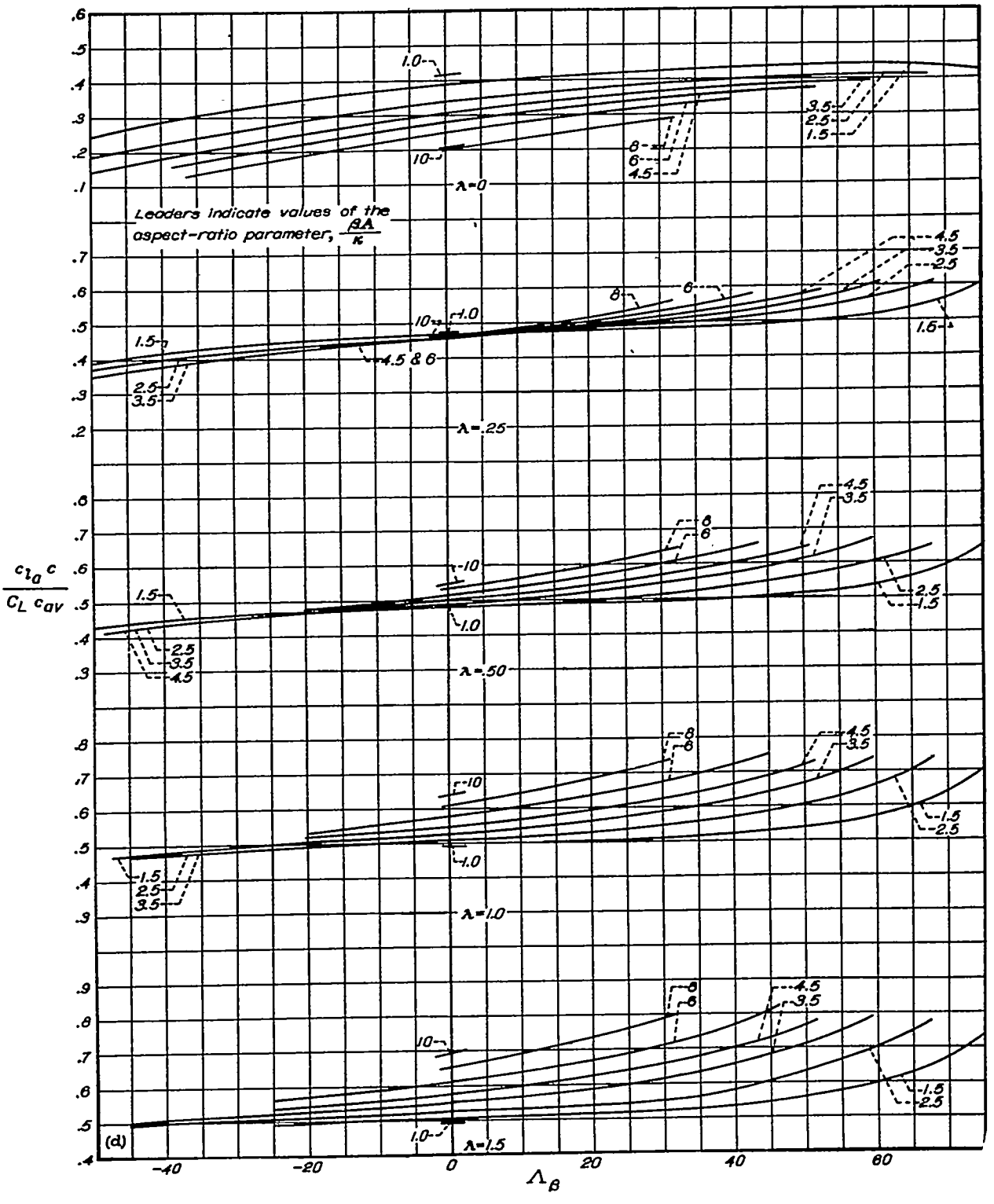

(d) Fraction of semispan, $\frac{2y}{b} = 0.9239$.

Figure 6.- Concluded.

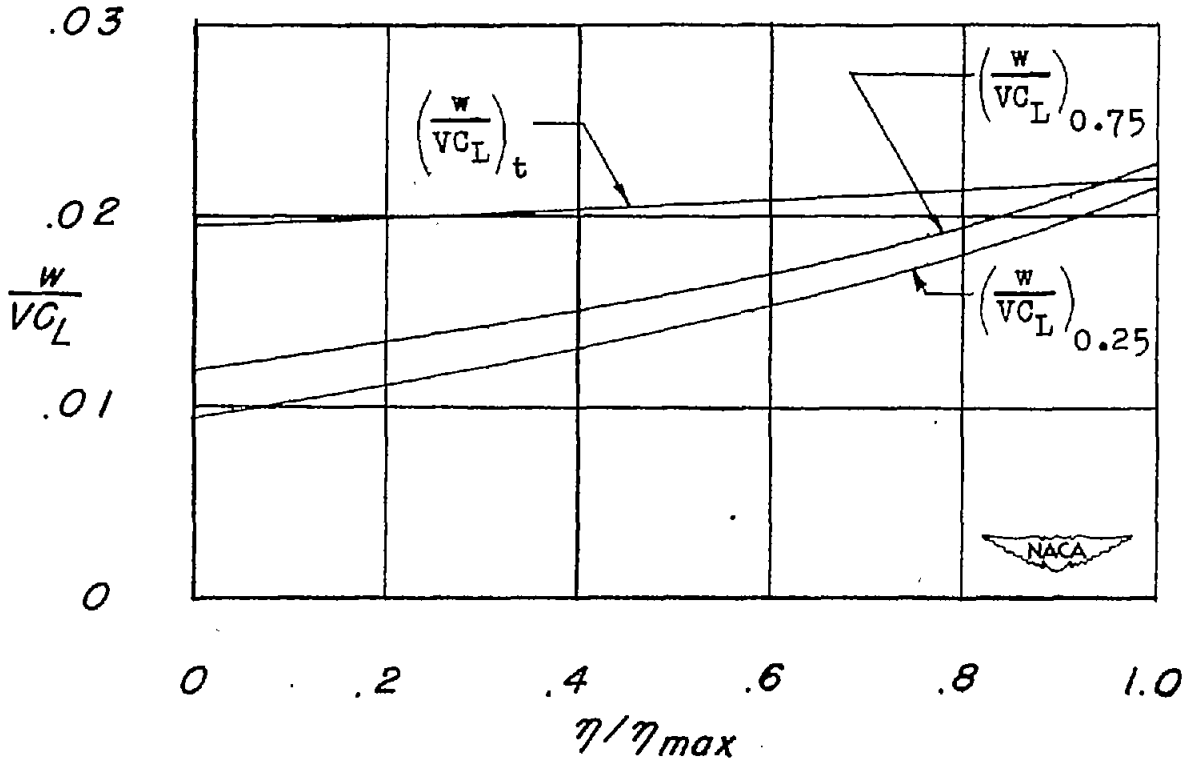

Figure 7.- Spanwise distribution of jet-boundary-induced angles due to wing lift.

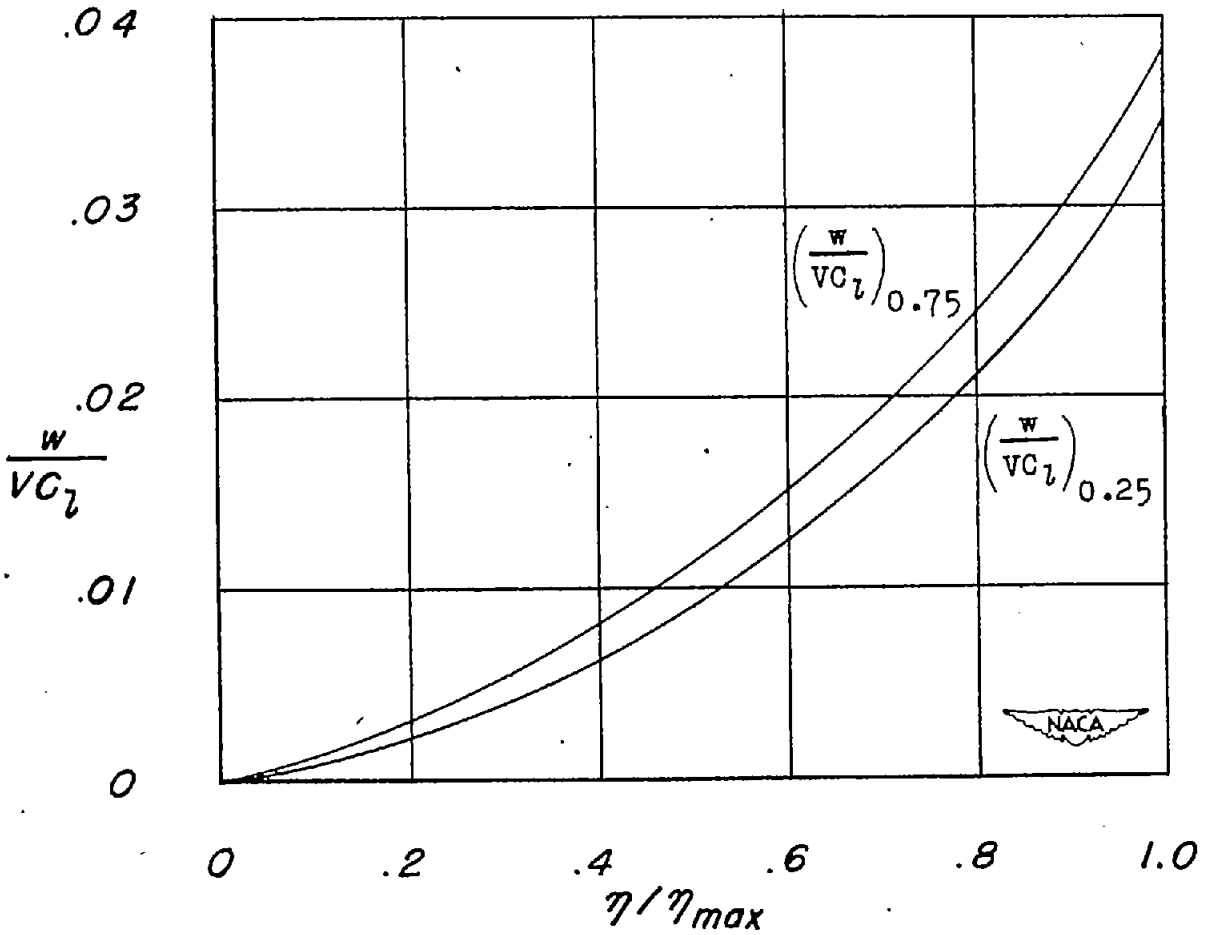

Figure 8.- Spanwise distribution of jet-boundary-induced angles due to aileron lift.

NACA-Langley - 8-6-53 - 1000